Article

Cell

Mutation of the Human Circadian Clock Gene *CRY1* in Familial Delayed Sleep Phase Disorder

Graphical Abstract

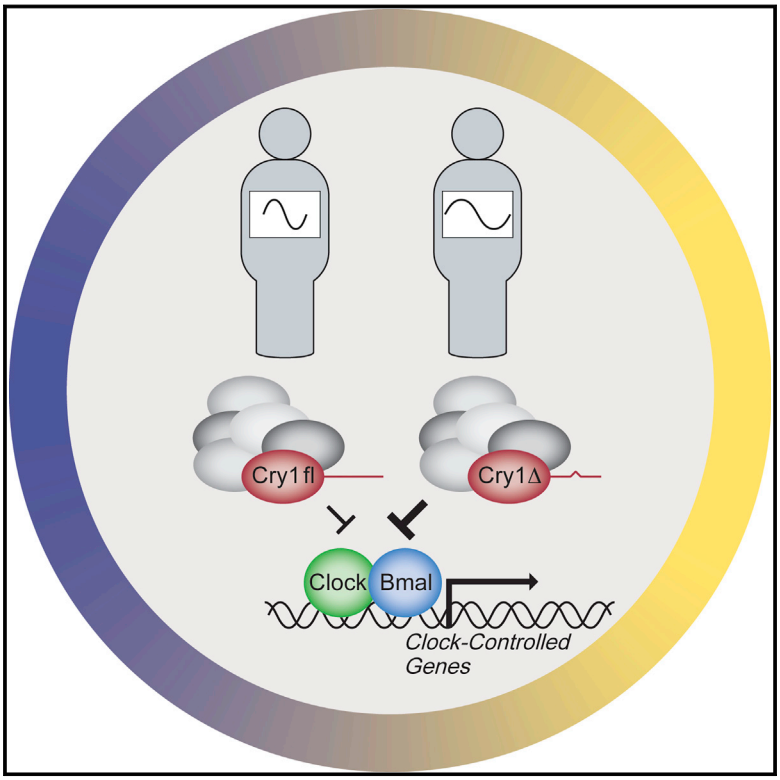

Authors

Alina Patke, Patricia J. Murphy, Onur Emre Onat, Ana C. Krieger, Tayfun Özçelik, Scott S. Campbell, Michael W. Young

Correspondence

patkea@rockefeller.edu (A.P.), young@mail.rockefeller.edu (M.W.Y.)

In Brief

A variation in the human circadian clock gene *CRY1* is associated with a familial form of delayed sleep phase disorder, providing genetic underpinnings for "night owls."

Highlights

- A human subject with DSPD with a variation in *CRY1* has altered circadian rhythms
- Proband kindred and unrelated carrier families display aberrant sleep patterns
- The allele alters circadian molecular rhythms
- The genetic variation enhances CRY1 function as a transcriptional inhibitor

Patke et al., 2017, Cell *169*, 203–215
April 6, 2017
http://dx.doi.org/10.1016/j.cell.2017.03.027

CellPress

Cell

Mutation of the Human Circadian Clock Gene *CRY1* in Familial Delayed Sleep Phase Disorder

Alina Patke,[1,*] Patricia J. Murphy,[2] Onur Emre Onat,[3] Ana C. Krieger,[4] Tayfun Özçelik,[3] Scott S. Campbell,[2] and Michael W. Young[1,5,*]

[1]Laboratory of Genetics, The Rockefeller University, New York, NY 10065, USA
[2]Laboratory of Human Chronobiology, Weill Cornell Medical College, White Plains, NY 10605, USA
[3]Department of Molecular Biology and Genetics, Faculty of Science, Bilkent University, Ankara 06800, Turkey
[4]Department of Medicine, Center for Sleep Medicine, Weill Cornell Medical College, New York, NY 10065, USA
[5]Lead Contact
*Correspondence: patkea@rockefeller.edu (A.P.), young@mail.rockefeller.edu (M.W.Y.)
http://dx.doi.org/10.1016/j.cell.2017.03.027

SUMMARY

Patterns of daily human activity are controlled by an intrinsic circadian clock that promotes ~24 hr rhythms in many behavioral and physiological processes. This system is altered in delayed sleep phase disorder (DSPD), a common form of insomnia in which sleep episodes are shifted to later times misaligned with the societal norm. Here, we report a hereditary form of DSPD associated with a dominant coding variation in the core circadian clock gene *CRY1*, which creates a transcriptional inhibitor with enhanced affinity for circadian activator proteins Clock and Bmal1. This gain-of-function *CRY1* variant causes reduced expression of key transcriptional targets and lengthens the period of circadian molecular rhythms, providing a mechanistic link to DSPD symptoms. The allele has a frequency of up to 0.6%, and reverse phenotyping of unrelated families corroborates late and/or fragmented sleep patterns in carriers, suggesting that it affects sleep behavior in a sizeable portion of the human population.

INTRODUCTION

The circadian clock is an internal self-sustained oscillator that operates in organisms' tissues and cells to align recurrent daily changes in physiology and behavior with 24-hr environmental cycles. In humans, dysfunction or misalignment of the circadian clock with environmental cues alters the timing of the sleep-wake cycle, leading to a variety of circadian rhythm sleep disorders (American Academy of Sleep Medicine, 2005). Delayed sleep phase disorder (DSPD), which is characterized by a persistent and intractable delay of sleep onset and offset times relative to the societal norm, represents the most commonly diagnosed type of circadian rhythm sleep disorder, with an estimated prevalence of 0.2%–10% in the general population (Zee et al., 2013). The wide range of prevalence estimates reflects heterogeneity in the manifestation of the disorder as well as variation in the stringency with which clinical diagnosis criteria are applied (Sack et al., 2007; Weitzman et al., 1981). The pathophysiology of DSPD remains obscure, with suspected causes including a differential susceptibility of an individual's circadian clock to environmental entrainment cues such as the light/dark cycle and altered properties of the oscillator itself that affect its period length (Aoki et al., 2001; Campbell and Murphy, 2007; Chang et al., 2009; Duffy et al., 2001; Micic et al., 2013).

The circadian clock is genetically encoded and susceptible to modification by spontaneous or targeted mutation of the respective factors in animal models (Crane and Young, 2014; Lowrey and Takahashi, 2011). In humans, rare genetic variations that shorten circadian period are linked to familial advanced sleep phase disorder (FASPD), a type of circadian rhythm sleep disorder with habitual sleep times earlier than the societal norm (Hirano et al., 2016; Toh et al., 2001; Xu et al., 2005, 2007). No comparable evidence has yet emerged for DSPD and the association of proposed genetic polymorphisms with late chronotype, and DSPD has remained controversial (Kripke et al., 2014). Yet, many classical twin studies have found a strong hereditary component to chronotype preference in the range of 40%–50%, arguing for an important role of genetic predisposition to DSPD etiology (Barclay et al., 2010; Hur et al., 1998; Koskenvuo et al., 2007; Vink et al., 2001). Here, we report a case of familial DSPD linked to a dominant coding variation in cryptochrome circadian clock 1 (*CRY1*). This association is maintained in unrelated carrier families of the *CRY1* variant. The studied allele encodes a CRY1 protein with an internal deletion, affecting its function as a transcriptional inhibitor and causing lengthening of the circadian period.

RESULTS

Characterization of Intrinsic Circadian Rhythmicity in the DSPD Proband

The clinical diagnosis of DSPD in the proband, subject "TAU11" (female, aged 46), was based on a sleep history and diagnostic interview, chronotype questionnaires, and actigraphy combined with a sleep log (Figure 1A). To better characterize the intrinsic circadian behavior, the subject completed an in-laboratory study during which sleep and core body temperature were continuously monitored (Figure 1B). The protocol consisted of a 2-day entrainment period with habitual sleep times derived from the sleep log. Entrained phase was determined by salivary dim light

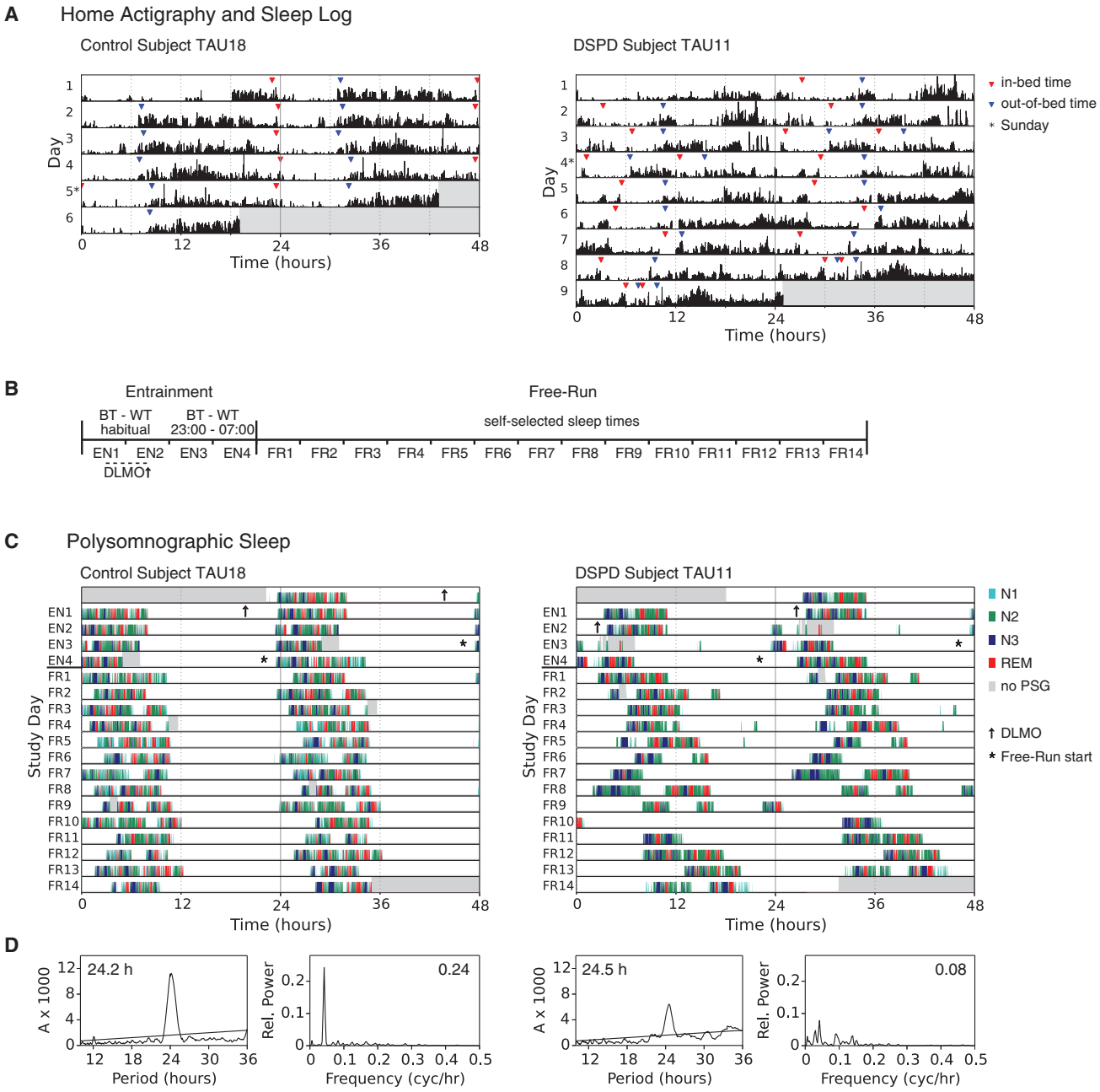

Figure 1. Circadian Behavior of Control Subject "TAU18" and the DSPD proband "TAU11"

(A) Double-plotted home actigraphy records. Red and blue triangles indicate in-bed/out-of-bed times, respectively, according to sleep logs. Asterisks indicate Sundays.

(B) In-laboratory protocol: entrainment conditions on the first 4 days with sleep-log-based, habitual sleep times on entrainment days (EN) 1 and 2 and enforced times in bed from 23:00 to 7:00 on EN3 and 4. Saliva samples for DLMO estimation were collected beginning at 18:00 on EN1 every 30 min until bedtime. From the fifth day on until the end of the study (free-run days FR1–14), subjects were kept under time-isolation conditions with instructions to sleep whenever so inclined. Polysomnographic (PSG) sleep and core body temperature were recorded continuously throughout the study.

(C) Double-plotted sleep/wake behavior during the in-laboratory study. Colors denote sleep stage derived from PSG records (N1, turquoise; N2, green; N3, blue; REM red). Gray areas indicate periods of missing PSG data during log-based time in bed. On the first and last study days, gray shading marks the beginning and end of data acquisition. Arrow denotes DLMO. Asterisk denotes the beginning of the free-run.

(D) Analysis of sleep rhythmicity. Circadian rhythm parameters during the free-run were analyzed by X^2 periodogram and fast Fourier transform (FFT) analysis, which yielded period and amplitude, respectively.

melatonin onset (DLMO) on the second entrainment night. This was followed by 2 days of enforced time in bed from 23:00 to 7:00. At the end of the 4-day entrainment interval, the subject entered a 14-day period of time isolation during which sleep was permitted whenever so inclined (free-run).

Compared to a control subject of normal chronotype undergoing the same protocol, several circadian abnormalities were apparent in the proband: consistent with a phase delay, entrained DLMO occurred at 2:32, well after the time expected in a subject of normal chronotype (typically between 20:00 and 22:00) and closer to the time of habitual sleep onset (Figure 1C) (Chang et al., 2009; Molina and Burgess, 2011). Sleep during the free-run was highly variable both in the timing and the duration of major sleep periods, consistent with at-home actigraphy and sleep-log records (Figures 1A and 1C). The resulting gross sleep/wake rhythm had a period of 24.5 hr with noticeably dampened amplitude (Figure 1D). By contrast, the 24.2-hr period length of a control subject undergoing the same protocol matches the intrinsic period length reported for normal human subjects (Czeisler et al., 1999). Aberrant rhythmicity in the sleep behavior of TAU11 was mirrored by the pattern of core body temperature oscillations in which a long-period rhythm of 24.8 hr and diminished amplitude were even more pronounced (Figures 2A–2C and S1). The phenotypic concordance of the different circadian measures strongly argues for the presence of an intrinsic circadian rhythm disorder in the proband.

Identification of CRY1 c.1657+3A>C as a Candidate DSPD Allele

To identify the cause of circadian dysfunction in the proband, we performed candidate sequencing of genes that form the circadian clock in mammals. The core molecular clock consists of a negative-feedback loop in which the activity of the transcription factors Clock and Bmal1 (called ARNTL in humans) is repressed by the products of its target genes of the Per and Cry family, creating a cycle that takes ~24 hr to complete (Figure 3A). In this complex process also involving regulation of post-translational modification and nuclear translocation, Cry1 is commonly recognized as the main transcriptional repressor of Clock and Bmal1 (Anand et al., 2013; Griffin et al., 1999; Kume et al., 1999; Oster et al., 2002; van der Horst et al., 1999; Vitaterna et al., 1999; Ye et al., 2014). By contrast, the mechanism of action of the Per proteins appears to be more variable, ranging from indirect repression through recruitment of generic chromatin modifiers to in fact promoting transcriptional de-repression (Chiou et al., 2016; Duong et al., 2011; Duong and Weitz, 2014). Our candidate gene sequencing identified an adenine-to-cytosine transversion within the 5′ splice site following exon 11 in one allele of the proband's *CRY1* gene (Figures 3B and 3C). Given usual conservation of the +3 position as a purine, this change is expected to cause splice site disruption and exon skipping (King et al., 1997). To test for a resulting coding change, we amplified part of the *CRY1* cDNA encompassing exon 11 from a primary dermal fibroblast cell line derived from the proband. Indeed, an additional product corresponding to the expected Δ11 size was present in the proband's sample, but not in those derived from 18 other unrelated subjects (Figure 3D). With a size of 72 base pairs, exon 11 skipping is predicted to cause an in-frame deletion of 24 residues in the C-terminal region of the CRY1 protein, and a matching, higher-mobility band was specifically detected in protein extracts from the proband cell line (Figure 3E).

Given the prominent role of CRY1 in the mammalian clock, we postulated that the circadian abnormalities in the proband were related to the observed modification of CRY1. To test this hypothesis, we obtained information on sleep patterns from members of the proband's family and genotyped them for presence or absence of the candidate allele. Delayed sleep behavior was found to be common among male and female family members and across several generations, consistent with an autosomal-dominant inheritance pattern (Figures 4A and S2; Table S1). Presence of the CRY1 c.1657+3A>C allele segregated with delayed sleep timing, with the exception of one carrier (TAUX08), who reported a history of persistent sleep problems but was complaint free at the time of study, on an occupationally required very early routine that was purposely maintained on free days (see Table S1 for details).

In a complementary approach, we also performed an unbiased search for genetic variants co-segregating with aberrant sleep behavior in the proband kindred through whole exome sequencing of additional family members (three affected, one unaffected). Among variants with minor allele frequencies below 1%, which are common to all affected subjects, but not the unaffected, and which are predicted to affect protein coding, the candidate *CRY1* allele was the only variant affecting a gene with a known or implicated role in the regulation of sleep or circadian rhythmicity (Table S2). Also, although some additional more common clock-gene variants were also present in the original proband TAU11, none of these segregated with sleep behavior in the family (see Methods Details). These results point to the CRY1 c.1657+3A>C allele as a strong candidate-genetic variant for familial DSPD.

Reverse Phenotyping of Sleep Behavior in Heterozygous and Homozygous Carriers of the CRY1 c.1657+3A>C Allele from an Unrelated Population

In databases of human genetic variation, the candidate *CRY1* allele has a frequency of up to 0.6% (rs184039278: minor allele frequency 0.0012 in 1000 Genomes, 0.004335 in ExAC total with 0.006537 in non-Finnish Europeans). This frequency lies within the reported range of DSPD prevalence (Zee et al., 2013) and is high enough to attempt the identification of additional carriers consenting to a characterization of their sleep behavior through a reverse-phenotyping approach (Özçelik and Onat, 2016). In genomic databases of the Turkish population, we identified 28 carriers of the CRY1 c.1657+3A>C allele, including one homozygous individual. Of these, investigation of sleep behavior through questionnaires and personal interview was possible in six unrelated families (DSPD-1, -2, -4, -6, -7, -9, and -14) totaling 70 subjects (8 homozygous carriers, 31 heterozygous carriers, 31 non-carriers) (Figure 5 and Table S1). Subjects also provided a DNA sample to determine the *CRY1* allele status. Aberrant sleep behavior was reported by 38 carriers, but not by their non-carrier relatives or spouses, indicating a very high penetrance of *CRY1*-related sleep disturbance consistent with the original proband family. In addition to late sleep times, a subset of carriers reported a pattern of fragmented

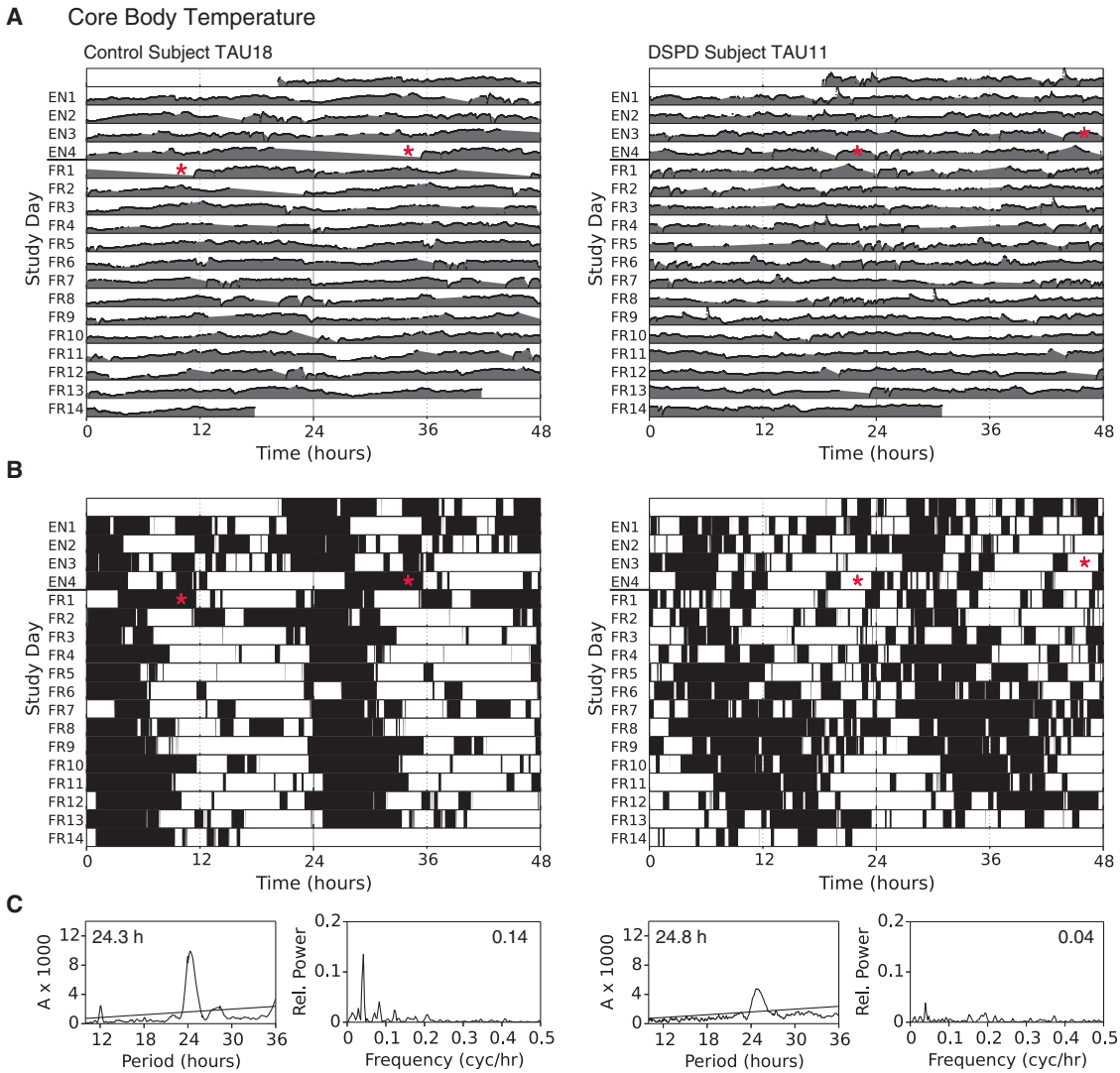

Figure 2. Core Body Temperature of Control Subject "TAU18" and the DSPD proband "TAU11"

(A) Double-plotted core body temperature during the in-laboratory study. The scale of the y axis for each individual study day is 2.3°C. Data shown as gray fill are interpolated from raw data shown as black dot overlay (see STAR Methods for details). Red asterisk in the DSPD proband denotes the beginning of the free-run. In the control subject, the indicated free-run start time corresponds to the time used for analysis of rhythmicity and differs from the actual free-run start time due to a preceding ~12-hr gap in the temperature record.

(B) Double-plotted sub-mean core body temperature. The mean temperature of the entire data series was calculated from outlier-corrected, interpolated data for each subject, and data points below the mean are plotted as black fill.

(C) Analysis of core body temperature rhythmicity. Circadian rhythmicity during the free-run was analyzed by X^2 periodogram and FFT analysis to measure period and amplitude, respectively.

See also Figure S1.

sleep consisting of a brief sleep period early in the night and extended naps during the day. Fragmented sleep was particularly prevalent among those carriers for whom early rising was a necessity due to cultural or social obligations. Of note, no difference in sleep behavior was observed between heterozygous and homozygous carriers of the *CRY1* allele, consistent with an autosomal-dominant mode of inheritance. The one carrier with reported conventional sleep times (DSPD-6 16-068) was subject to work-imposed strong light exposure, raising the possibility that the *CRY1*-mediated disposition can be modifiable given adequate environmental conditions. Nevertheless, there was a very strong association between *CRY1* allele status and sleep behavior in the reverse-phenotyped families and the original proband kindred (Fisher's exact $p < 0.0001$, odds ratio = 1,928, 95% confidence interval 76–48,904).

CRY1 Exon 11 Deletion Affects Circadian Clock Cycling and CRY1 Molecular Function

To directly test whether the deletion of exon 11 of *CRY1* affects the circadian clock, we created cell lines differing only in the

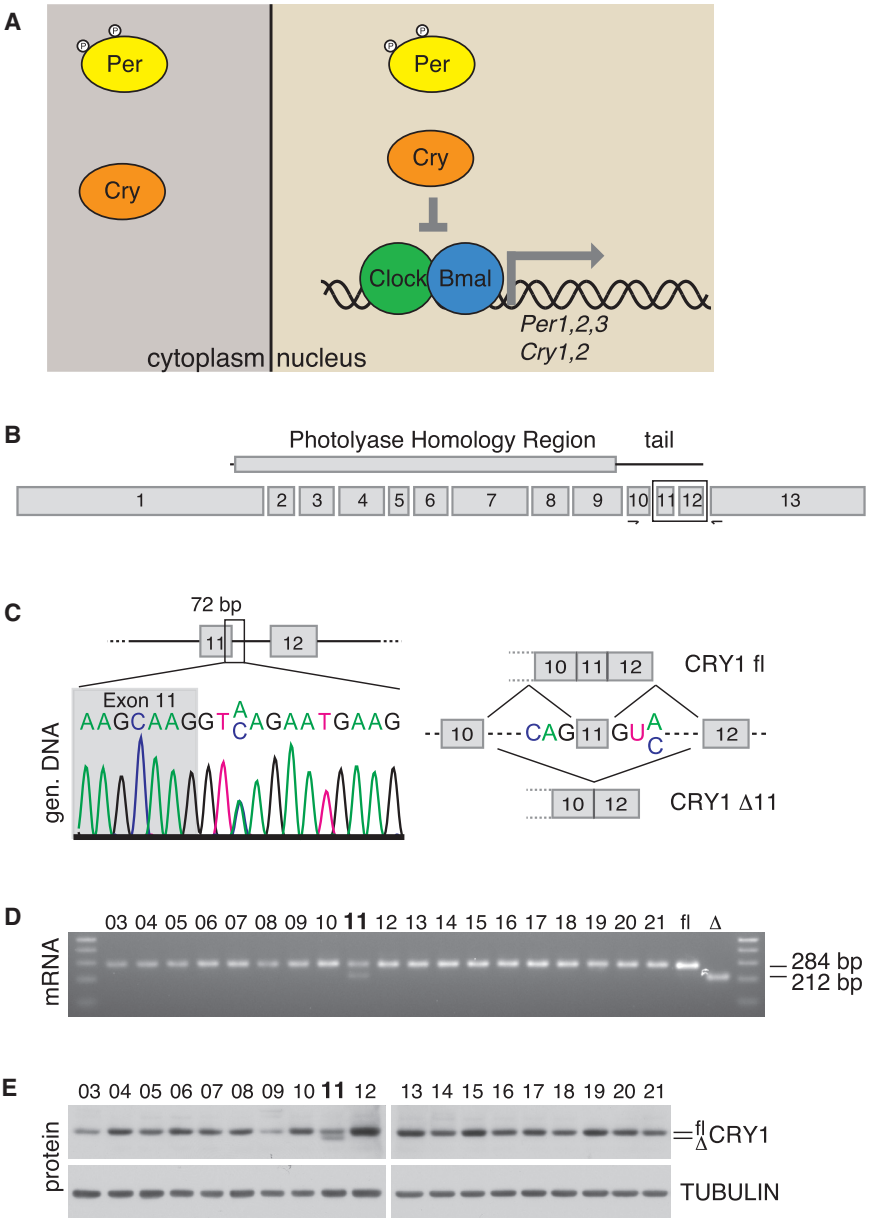

Figure 3. Mutation of *CRY1*

(A) The core molecular circadian clock in mammals. Transcriptional activity of Clock and Bmal1 leads to expression of Per and Cry family genes, whose products undergo posttranslational modification, translocate to the nucleus, and inhibit Clock/Bmal1-mediated transcription with Cry1 acting as the main repressor.

(B) Exon organization of the human *CRY1* gene with the encoded protein regions shown above. Box represents the region enlarged in (C). Arrows indicate primer binding sites used in (D).

(C) Primary sequencing trace of the region immediately following exon 11 in the proband's genomic DNA (left) and schematic diagram depicting the expected consequences of the A-to-C transversion on *CRY1* mRNA splicing (right).

(D) RT-PCR analysis of the *CRY1* mRNA between exons 10 and 13. Samples 03 to 21 are amplified from primary fibroblast cell lines from 19 different subjects, with number 11 belonging to the proband. Controls on the right are amplified from cloned *CRY1* full-length and Δ11 cDNA. Expected product sizes are indicated.

(E) CRY1 protein expression in the 19 subject-derived fibroblast cell lines. TUBULIN levels are shown as a loading control.

expressed CRY1 form. Human full-length or CRY1 Δ11 variants were expressed in *CRY1/2* double-deficient mouse embryonic fibroblasts (DKO MEFs) using regulatory elements previously characterized to recapitulate endogenous CRY1 oscillation (Ukai-Tadenuma et al., 2011). As expected, CRY1 expression restored circadian cycling of a Bmal-luciferase reporter in previously arrhythmic DKO MEFs, albeit with a long period, as previously described for this experimental system (Khan et al., 2012) (Figure 4B). Compared to full-length CRY1, expression of the Δ11 form increased circadian period by approximately half an hour, similar to the phenotype observed in the proband. The effect was not due to differences in the amounts of the ectopically expressed CRY1 forms (Figure 4B). In contrast to CRY1, expression of CRY2 in CRY DKO MEFs did not restore their circadian rhythmicity, consistent with previous reports (Khan et al., 2012), and the differential period length between the two CRY1 forms was still observed in its presence (Figure S3A). These results demonstrate a direct effect of *CRY1* exon 11 deletion on circadian period length, which matches DSPD symptoms.

The Cry1 protein consists of a conserved photolyase homology region, which mediates transcriptional repression of Clock/Bmal1, a C-terminal helix previously described as a predicted coiled coil, which interacts with Per2 and Fbxl3 in a mutually exclusive manner and a C-terminal extension also referred to as the "tail" (Figures 3B and S3B) (Chaves et al., 2011; Merbitz-Zahradnik and Wolf, 2015). The Cry1 tail region represents the most poorly conserved and least functionally and structurally characterized region of the protein. It has been shown to affect Cry1 nuclear translocation, to interact with the Bmal1 transactivation domain possibly in an acetylation-dependent fashion, and to be phosphorylated in a manner that involves regulation by DNA-PK (Chaves et al., 2006; Czarna et al., 2011; Gao et al., 2013; Hirayama et al., 2007; Xu et al., 2015). Interestingly, the tail is not essential to Cry1's ability to restore circadian cycling to arrhythmic DKO MEFs but does modulate the period length and amplitude of the resulting oscillation (Khan et al., 2012; Li et al., 2016). Overall, current evidence points to a regulatory role of the Cry1 tail in the transcriptional repression complex involving Clock, Bmal1, and possibly other factors at

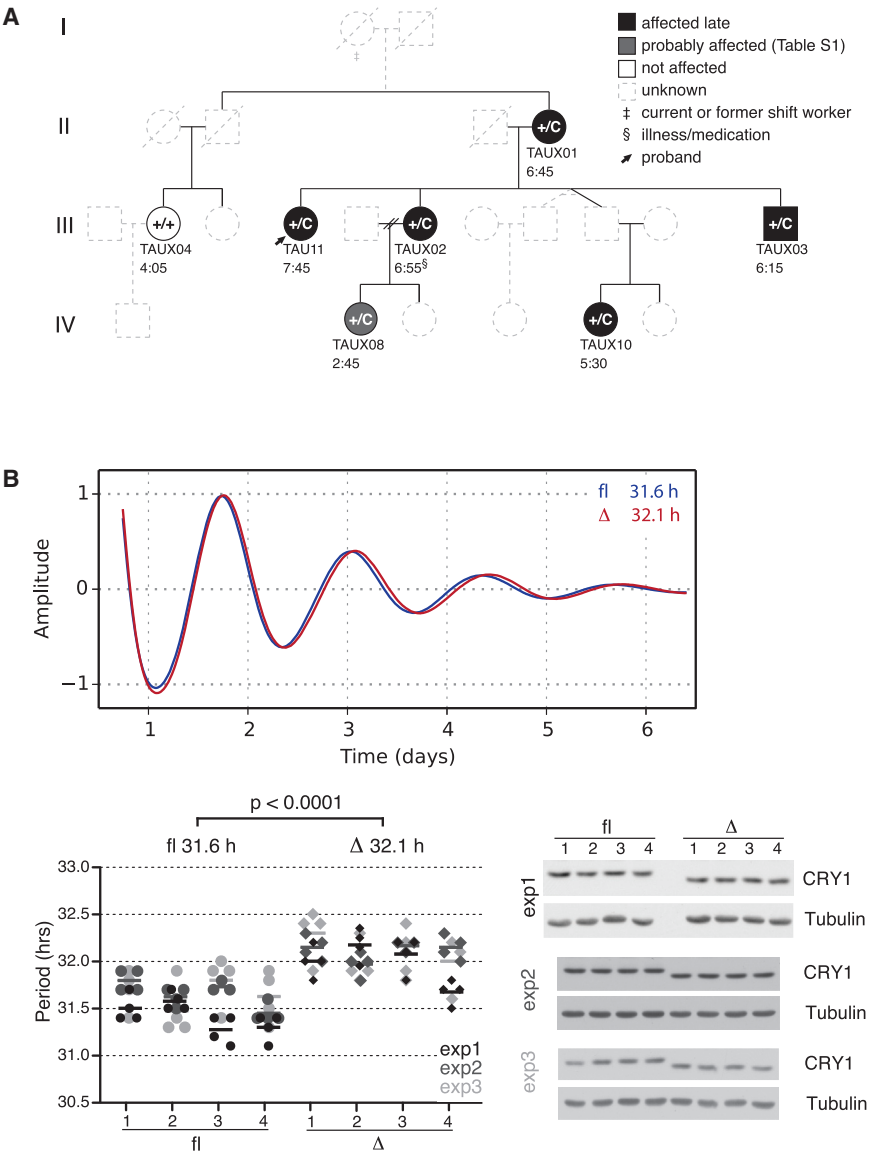

Figure 4. Effect of the *CRY1* Mutation on Human Sleep Timing and Clock Oscillation

(A) Segregation of the CRY1 c.1657+3A>C allele with delayed sleep in the proband's family. Genotype is shown inside symbols. Color code and symbols are explained in the legend. Numbers represent midsleep point on free days (MSF) (Roenneberg et al., 2003). See also Table S1 for details.

(B) Deletion of CRY1 exon 11 affects circadian period length. *CRY1* fl or Δ11 cDNAs were expressed in Bmal1-luc DKO MEFs using a lentiviral expression system that preserved the regulatory elements necessary to recapitulate endogenous CRY1 expression. Cells were synchronized with 20 μM forskolin, and bioluminescence output was recorded for ~7 days. Traces show average detrended bioluminescence counts normalized to the first peak for each genotype (CRY1 fl blue, CRY1 Δ11 red). Period was calculated from bioluminescence recordings of quadruplicate samples from quadruplicate CRY1 infections (circles, fl 1–4; diamonds, Δ 1–4). Data from three independent experiments are shown (gray shading). Mean periods from each infection (indicated by horizontal lines) were used to assess statistical significance between genotypes. The overall mean period was 31.6 hr for full-length CRY1 and 32.1 hr for Δ11 CRY1. Steady-state CRY1 levels for infections 1–4 from each experiment were measured by western blot with Tubulin shown as loading control.

See also Figures S2 and S3 and Table S1.

various stages of the circadian cycle. Deletion of exon 11 results in the removal of 24 residues from the CRY1 C-terminal tail. In accordance with previous functional characterizations of the Cry1 protein regions, we did not observe a difference in the capacity of CRY1 Δ11 to inhibit Clock/Bmal1-dependent transcription of an E-box-driven luciferase reporter plasmid in heterologous cell-based assays, which do not require the Cry1 tail (Chaves et al., 2006; Khan et al., 2012) (Figures S3C and S3D). Further, although some modifications within the tail region can affect the half-life of the Cry1 protein under certain conditions (Gao et al., 2013), we did not observe gross differences in the stability of CRY1 Δ11 versus the full-length form in the subject's primary fibroblasts (Figure S3E), and luciferase fusion proteins with the respective CRY1 forms decayed at a similar rate (Figure S3F).

The existence of a nuclear localization signal in the Cry1 tail, albeit C-terminal to the exon 11 region, prompted us to assess the subcellular distribution of the different CRY1 forms. Unexpectedly, deletion of exon 11 increased CRY1 abundance in the nuclear fraction of the proband's fibroblasts throughout the circadian cycle (Figures 6A and S4A). This increased abundance was not caused by potential additional variations in the proband's cells but represents an intrinsic property of the modified CRY1 protein, as enhanced CRY1 Δ11 nuclear localization was also observed in DKO MEFs engineered to express both CRY1 forms (CRY1 fl/Δ MEFs) (Figures 6B and S4B).

CRY1 Δ11 Shows Enhanced Interactions with Clock and Bmal1 Proteins

Preferential nuclear localization of CRY1 Δ11 led us to assess its binding to its target transcription factors Clock and Bmal1. Although both CRY1 forms present in the subject's fibroblasts were found to be capable of interaction, the fraction of CRY1 immunoprecipitating with ARNTL or Clock was enriched for the Δ11 form (Figures 6C and S4C). This is not solely a reflection of differential subcellular distribution as ARNTL or Clock immunoprecipitated from purified nuclear extracts still bound more Δ11 than full-length CRY1. Enhanced interaction with the CRY1 Δ11 form was replicated in CRY1 fl/Δ MEFs independent

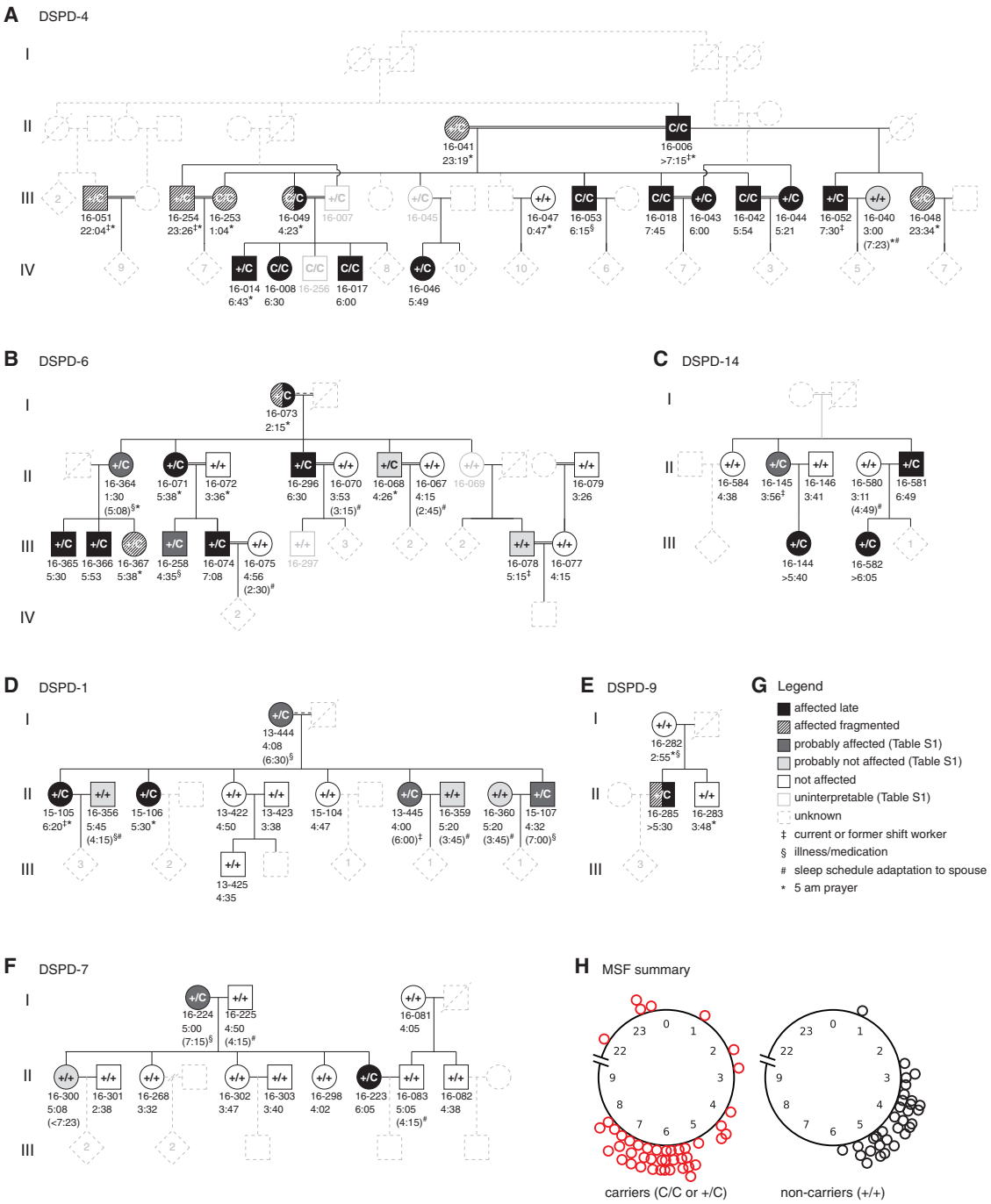

Figure 5. Sleep Behavior in CRY1 c.1657+3A>C Carrier Families of Turkish Descent

(A–F) Sleep behavior in families DSPD-4, -6, -14, -1, -9, and -7 assessed through sleep and chronotype questionnaires and personal interview. Genotype is shown inside symbols. Numbers represent mid-sleep point on free days (MSF) (Roenneberg et al., 2003). See also Table S1 for details.

(G) Legend for colors and symbols used in (A–F).

(H) MSF from subjects in (A–F) as well as Figure 4A are plotted on a discontinuous clock face from 22:00 to 9:00 for carriers (left, red) and non-carriers (right, black). No subject data fell within the gap time (9:00 to 22:00) not represented in the plot.

of circadian phase (Figures 6D and S4D). Interestingly, although exon 11 partially overlaps with a region in the Cry1 tail that has been identified as a binding site for the Bmal1 transactivation domain acetylated at lysine 538, we still observed preferential binding of CRY1 Δ11 to acetylated Bmal1. We also consistently detected higher overall levels of acetyl-Bmal1 in control DKO

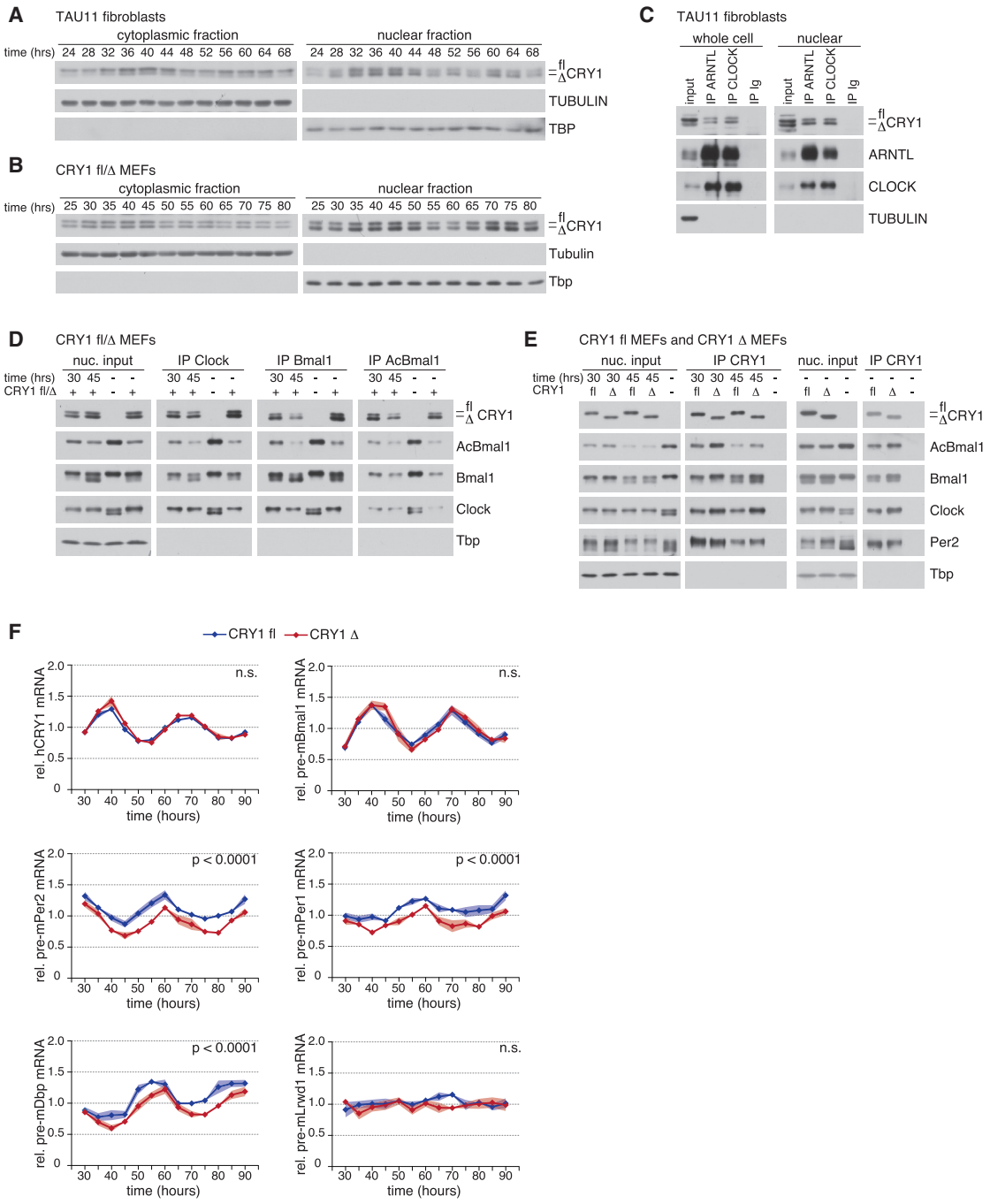

Figure 6. Exon 11 Deletion Enhances CRY1 Function in the Molecular Circadian Clock

(A) CRY1 expression was assessed in fractionated extracts prepared from the proband's fibroblasts at the indicated times following synchronization. TUBULIN and TBP were used as loading controls for cytoplasmic and nuclear extracts, respectively, and to assess fractionation purity.

(B) Same as (A) except proband fibroblasts were replaced with CRY1 fl/Δ MEFs, and the sampling interval was adjusted to account for the longer circadian period in this cell type.

(C) Co-immunoprecipitation of CRY1 with ARNTL and CLOCK in unsynchronized whole-cell (left) and nuclear (right) extracts from the proband's fibroblasts.

(D) Co-immunoprecipitation of CRY1 with Clock, Bmal1, and K538 Acetyl-Bmal1 in nuclear extracts from CRY1 fl/Δ MEFs at 30 or 45 hr post-synchronization as well as from unsynchonized CRY1 fl/Δ and empty vector control DKO MEFs.

(E) Co-immunoprecipitation of Clock, Bmal1, K538 Acetyl-Bmal1, and Per2 with CRY1 from nuclear extracts of CRY1 fl or Δ11 MEFs at 30 or 45 hr post-synchronization as well as from unsynchronized CRY1 fl or Δ11 MEFs and the empty vector control.

(legend continued on next page)

MEFs, which only received empty vector and remained devoid of cryptochromes, potentially indicating a more complex role of Bmal1 acetylation than currently suggested. Selective expression of either the full-length or the CRY1 Δ11 form in DKO MEFs allowed us to assess CRY1 binding to its interaction partners in reciprocal immunoprecipitations of the respective CRY1 form. Consistent with our other findings, more Clock, acetyl-Bmal1, and total Bmal1 immunoprecipitated with CRY1 Δ11 than with the full-length protein (Figures 6E and S4E). At the same time, the levels of CRY1-associated Per2 remained similar between the two CRY1 forms, suggesting the presence of separate CRY1-containing protein complexes with differential susceptibility to exon 11 deletion. Together, these results demonstrate that, rather than disabling CRY1, deletion of exon 11 enhances its presence in the nucleus and the binding to its target transcription factors, properties that are expected to promote its function as a transcriptional inhibitor.

CRY1 Δ11 Strengthens Transcriptional Inhibition

To directly test whether CRY1 Δ11 acts as a more potent transcriptional inhibitor during the intact clock cycle, we compared the expression of selected target genes in our engineered cell lines expressing either full length or CRY1 Δ11. As expected, cyclic CRY1 expression restored the circadian oscillation of *pre-Bmal1*, *pre-Per2*, *pre-Per1*, and *pre-Dbp* mRNAs with a long-period rhythm, although the sampling interval impeded an accurate determination of period length, as previously achieved by the high-resolution luciferase assay (Figure 6F). Compared to CRY1 full-length cells, the levels of *pre-Per2*, *pre-Per1*, and *pre-Dbp* mRNAs were reduced in CRY1 Δ11 cells, demonstrating stronger repression of Clock/Bmal1-mediated transcription by CRY1 Δ11 consistent with its other properties. In contrast, expression of *pre-Bmal1*, which is controlled by a different set of regulatory elements (Preitner et al., 2002; Ueda et al., 2002), remained unaffected by the CRY1 modification, as did the levels of a non-circadian control gene.

Given enhanced association with the target transcription factors as well as reduced expression of the relevant transcripts, we wondered whether exon 11 deletion affected CRY1 occupancy at its target gene promoters. In the circadian transcriptional feedback loop, repression can occur by blocking of the DNA-bound transcription factors or by their displacement and sequestration away from DNA (Menet et al., 2010). Cry1-dependent inhibition of gene expression has been shown to involve both of these modes (Ye et al., 2014). Using our cell lines engineered to selectively express full length or CRY1 Δ11, we measured the binding of CRY1, Bmal1, and Clock to target regions in the *Per2* and *Dbp* promoters by chromatin immunoprecipitation (Figures 7A–B). At the time of high Bmal1/low Per2 expression, reduced promoter association of CRY1, Bmal1, and Clock was observed in cells expressing CRY1 Δ11 compared to the full-length form, while the association of the control histone 3 trimethylated at lysine 4 (H3K4me3) remained unaltered. As expected, in control reactions measuring a non-circadian promoter, only H3K4me3 binding was observed while the amounts of CRY1, Bmal1, and Clock were at or near the background levels of the assay (Figure 7C). These results demonstrate that CRY1 exon 11 deletion specifically reduces the presence of clock gene proteins at target gene promoters, consistent with Cry1-mediated transcriptional regulation through displacement of Clock and Bmal1.

DISCUSSION

As the major transcriptional inhibitor in the negative feedback loop that constitutes the core molecular clock, Cry1 represents a critical regulator of circadian period length. In general, there is a positive correlation between the amount of Cry1 and period length, although exceptions to this rule can occur upon manipulation of selected protein regions (Busino et al., 2007; Godinho et al., 2007; Hirota et al., 2012; Ode et al., 2016; Oshima et al., 2015; Siepka et al., 2007; van der Horst et al., 1999; Vitaterna et al., 1999; Zhang et al., 2009). Moreover, period length has been shown to correlate with the affinity of Cry1 to Bmal1 (Xu et al., 2015).

Our results show that the *CRY1* DSPD allele represents a gain-of-function mutation with deletion of exon 11 leading to increased CRY1 nuclear localization, enhanced interaction with the transcription factors Clock and Bmal1, their displacement from chromatin, and heightened inhibition of their target genes (Figure S5). Expression of this more potent CRY1 form (CRY1 Δ11) is associated with a lengthened period of molecular circadian rhythms in cells. A human carrier of *CRY1 Δ11* studied in temporal isolation displayed corresponding, long-period behavioral and body-temperature rhythms with diminished amplitudes. These phenotypic changes are consistent with the established positive correlation of period length with CRY1 availability and affinity to its target transcription factors, thus providing a mechanistic explanation for the development of DSPD in carriers of the *CRY1 Δ11* allele.

The stronger inhibitory function of the CRY1 Δ11 variant is only observed in the context of an intact clock cycle, raising interesting questions regarding the mechanism by which the CRY1 protein tail influences Clock/Bmal1 transcriptional activity. While currently available structural characterizations of the mammalian cryptochrome proteins have been insightful regarding their binding to Per2 and Fbxl3, the interaction with their target transcription factors has yet to be visualized, and none of the structures includes the Cry1 tail region (Merbitz-Zahradnik and Wolf, 2015). It is conceivable that the tail could affect transcription factor/repressor interaction through regulated binding to the CRY1 photolyase homology region or Clock/Bmal1, causing conformational changes to the complex. Such an event could be temporally controlled through recruitment or loss of additional complex components, through inducible post-translational modification of any of the proteins, or through changes to the CRY1 protein such as its redox state or the presence of cofactors, including flavin adenine dinucleotide or zinc ions. While

(F) Levels of *CRY1*, *pre-Bmal1*, *pre-Per2*, *pre-Per1*, *pre-Dbp*, and *pre-Lrwd1* were assessed by real-time quantitative RT-PCR in synchronized CRY1 fl (blue) or Δ11 (red) MEFs. Graphs show mean expression levels from five independent experiments, with the shaded area indicating the standard error. Statistically significant differences in gene expression between genotypes are indicated. n.s., not significant.
See also Figure S4.

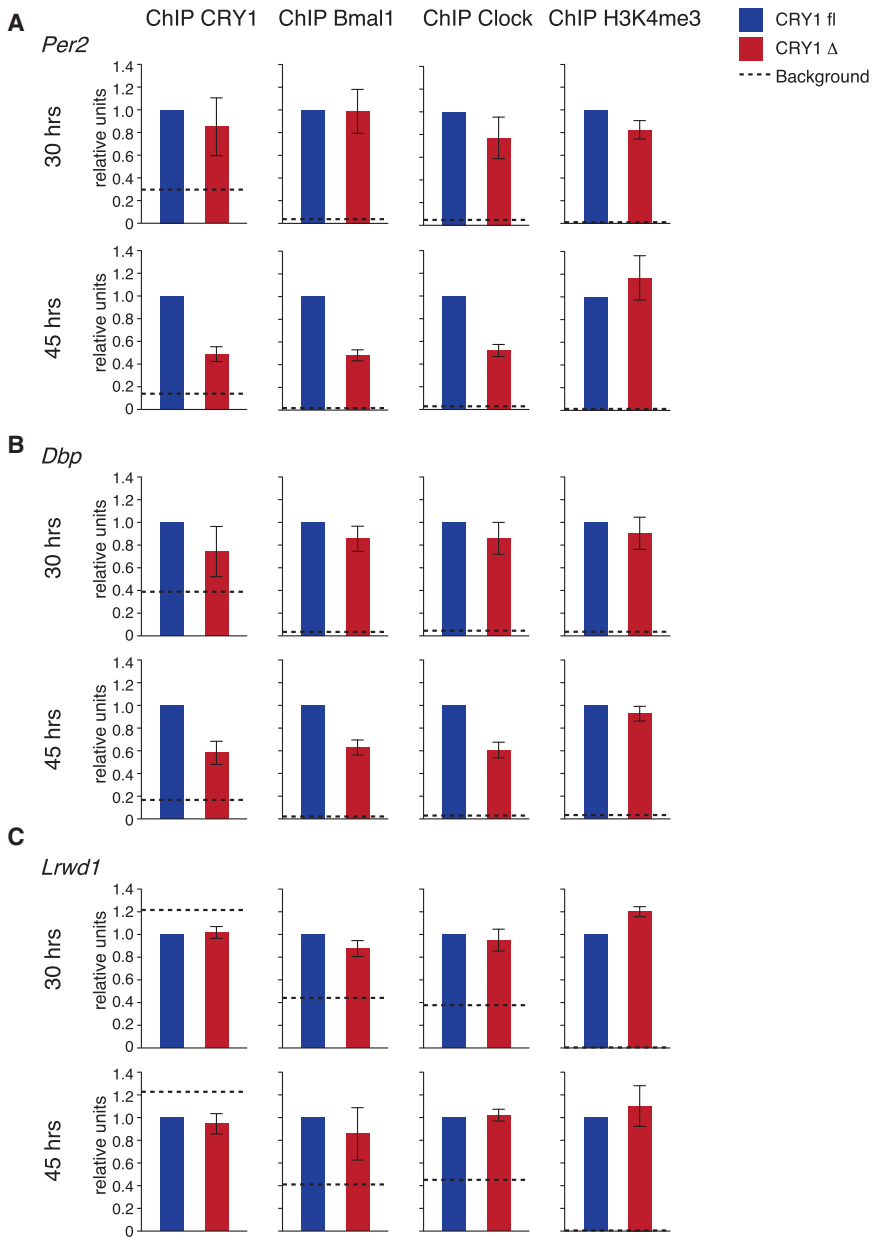

Figure 7. CRY1 Δ11 Affects the Occupancy of CRY1, Bmal1, and Clock at Target Gene Promoters

(A–C) CRY1, Bmal1, Clock, and H3K4me3 were immunoprecipitated from CRY1 fl (blue) or Δ11 (red) MEFs at 30 or 45 hr post-synchronization following chromatin crosslinking. The amount of *Per2*- (A), *Dbp*- (B), and *Lrwd1*-promoter DNA (C) in the immunoprecipitates was assessed by real-time quantitative PCR. The background signal (dashed line) corresponds to the respective real-time quantitative PCR values of a control reaction using a CRY1 chromatin-immunoprecipitate from Cry-deficient cells as template. Data in each experiment were normalized to the amount in the CRY1 fl sample, which was set to 1. Error bars represent the standard error from three independent experiments.

dispensable for basic repression, the CRY1 tail could thus exert the capacity to modulate transcriptional inhibition at defined stages of the circadian cycle.

In our analyses of cellular circadian rhythms, the *CRY1 Δ11* allele consistently lengthened the period of molecular oscillations by approximately half an hour. Earlier work has demonstrated a strong relationship between circadian period, entrained phase, and sleep timing in humans, such that moderate changes in period are associated with much larger shifts in the relative phases of bedtime and the evening increase in serum melatonin (Gronfier et al., 2007; Wright et al., 2005). Accordingly, a half-hour change in the period of the human circadian clock is expected to change the relationship of sleep timing and evening melatonin onset (DLMO) by ~2–2.5 hr. These predictions agree well with the behavioral and physiological findings we have presented.

Databases of human genetic variation report a frequency between 0.1% and 0.6% for the CRY1 c.1657+3A>C allele, such that up to 1 in 75 members of certain populations could carry the dominant *CRY1* variant. Our analyses of the original proband family as well as a large number of subjects from unrelated families of completely different ethnicity show that both homo- and heterozygous CRY1 c.1657+3A>C carrier status is strongly associated with late sleep times and sleep fragmentation. Possibly, the latter behavior may be a manifestation of carrier allele status under environmental conditions that do not accommodate late sleep times, as can often be the case due to cultural, social, or professional obligations. Alternatively, inter-individual differences in genetic background or exposure to environmental entrainment signals may affect the nature and penetrance of sleep disturbances in *CRY1 Δ11* allele carriers, and similar phenomena have been observed in both human and animal studies of circadian rhythmicity (Azzi et al., 2014; Pittendrigh and Daan, 1976; Shimomura et al., 2013; Toh et al., 2001). The *CRY1 Δ11* variant may thus lead to a broader range of sleep-disorder phenotypes with delay being the most common manifestation.

STAR★METHODS

Detailed methods are provided in the online version of this paper and include the following:

- KEY RESOURCES TABLE

SUPPLEMENTAL INFORMATION

Supplemental Information includes five figures and three tables and can be found with this article online at http://dx.doi.org/10.1016/j.cell.2017.03.027.

AUTHOR CONTRIBUTIONS

A.P., P.J.M., S.S.C., and M.W.Y. conceived of the project. P.J.M. and S.S.C. designed experiments and collected data for Figures 1, 2, 4A, S1, and S2. A.P. and M.W.Y. analyzed data for Figures 1, 2, 4A, S1, and S2 with input from P.J.M., A.C.K. and S.S.C. A.P. designed and performed experiments in Figures 3, 4B, 6, 7, S3, and S4. O.E.O. and T.Ö. collected data for Figure 5. A.P., O.E.O., T.Ö., and M.W.Y. analyzed data for Figure 5. A.P. prepared all figures and wrote the manuscript with input from all authors. A.P., T.Ö., S.S.C., and M.W.Y. secured funding.

ACKNOWLEDGMENTS

We thank the human study participants; the technical staff of the Laboratory of Human Chronobiology; Adam Savitz for conducting physical exams; Mary Morton for obtaining skin biopsies; Melanie Roberts for recruiting and obtaining data from the proband's family; Boris Dubrovsky for scoring polysomnography records; Nazlı Başak, Ali Dursun, Uğur Özbek, Köksal Özgül, and Bülent Yıldız for establishing initial contact to Turkish DSPD families; Hiroki Ueda, Steve Kay, and Steven Reppert for reagents; Avinash Abhyankar and the New York Genome Center for help with whole exome sequencing; Jeffrey Friedman for discussion and help with subject identification; Philip Kidd for help with processing of raw core body temperature data; the Friedman and Tarakhovsky laboratories for generously sharing equipment; and Cori Bargmann, Joseph Gleeson, André Hoelz, and Leslie Vosshall for comments on the manuscript. This work was supported by NIH grant RO1 NS052495 (S.S.C.), a sub-award #12081164 of NS052495 provided by Weill Cornell Medical College (M.W.Y.), Calico Life Sciences LLC (M.W.Y.), The Rockefeller University Center for Clinical and Translational Science grants UL1 TR000043 and UL1 TR001866 (A.P.), the Turkish Academy of Sciences-TÜBA (T.Ö.), The Rockefeller University Women & Science Postdoctoral Fellowship program (A.P.), and a NARSAD Young Investigator Grant #21131 from the Brain & Behavior Research Foundation (A.P.). P.J.M is currently employed by Eisai Inc.

Received: January 14, 2017
Revised: February 18, 2017
Accepted: March 20, 2017
Published: April 6, 2017

REFERENCES

American Academy of Sleep Medicine (2005). International Classification of Sleep Disorders: Diagnostic and Coding Manual, Second Edition (Westchester, Illinois: American Academy of Sleep Medicine).

Anand, S.N., Maywood, E.S., Chesham, J.E., Joynson, G., Banks, G.T., Hastings, M.H., and Nolan, P.M. (2013). Distinct and separable roles for endogenous CRY1 and CRY2 within the circadian molecular clockwork of the suprachiasmatic nucleus, as revealed by the Fbxl3(Afh) mutation. J. Neurosci. *33*, 7145–7153.

Aoki, H., Ozeki, Y., and Yamada, N. (2001). Hypersensitivity of melatonin suppression in response to light in patients with delayed sleep phase syndrome. Chronobiol. Int. *18*, 263–271.

Archer, S.N., Robilliard, D.L., Skene, D.J., Smits, M., Williams, A., Arendt, J., and von Schantz, M. (2003). A length polymorphism in the circadian clock gene Per3 is linked to delayed sleep phase syndrome and extreme diurnal preference. Sleep *26*, 413–415.

Azzi, A., Dallmann, R., Casserly, A., Rehrauer, H., Patrignani, A., Maier, B., Kramer, A., and Brown, S.A. (2014). Circadian behavior is light-reprogrammed by plastic DNA methylation. Nat. Neurosci. *17*, 377–382.

Barclay, N.L., Eley, T.C., Buysse, D.J., Archer, S.N., and Gregory, A.M. (2010). Diurnal preference and sleep quality: same genes? A study of young adult twins. Chronobiol. Int. *27*, 278–296.

Benloucif, S., Burgess, H.J., Klerman, E.B., Lewy, A.J., Middleton, B., Murphy, P.J., Parry, B.L., and Revell, V.L. (2008). Measuring melatonin in humans. J. Clin. Sleep Med. *4*, 66–69.

Brown, S.A., Fleury-Olela, F., Nagoshi, E., Hauser, C., Juge, C., Meier, C.A., Chicheportiche, R., Dayer, J.M., Albrecht, U., and Schibler, U. (2005). The period length of fibroblast circadian gene expression varies widely among human individuals. PLoS Biol. *3*, e338.

Busino, L., Bassermann, F., Maiolica, A., Lee, C., Nolan, P.M., Godinho, S.I., Draetta, G.F., and Pagano, M. (2007). SCFFbxl3 controls the oscillation of the circadian clock by directing the degradation of cryptochrome proteins. Science *316*, 900–904.

Campbell, S.S., and Murphy, P.J. (2007). Delayed sleep phase disorder in temporal isolation. Sleep *30*, 1225–1228.

Chang, A.M., Reid, K.J., Gourineni, R., and Zee, P.C. (2009). Sleep timing and circadian phase in delayed sleep phase syndrome. J. Biol. Rhythms *24*, 313–321.

Chaves, I., Pokorny, R., Byrdin, M., Hoang, N., Ritz, T., Brettel, K., Essen, L.O., van der Horst, G.T., Batschauer, A., and Ahmad, M. (2011). The cryptochromes: blue light photoreceptors in plants and animals. Annu. Rev. Plant Biol. *62*, 335–364.

Chaves, I., Yagita, K., Barnhoorn, S., Okamura, H., van der Horst, G.T., and Tamanini, F. (2006). Functional evolution of the photolyase/cryptochrome protein family: importance of the C terminus of mammalian CRY1 for circadian core oscillator performance. Mol. Cell. Biol. *26*, 1743–1753.

Chiou, Y.Y., Yang, Y., Rashid, N., Ye, R., Selby, C.P., and Sancar, A. (2016). Mammalian Period represses and de-represses transcription by displacing

CLOCK-BMAL1 from promoters in a Cryptochrome-dependent manner. Proc. Natl. Acad. Sci. USA *113*, E6072–E6079.

Ciarleglio, C.M., Ryckman, K.K., Servick, S.V., Hida, A., Robbins, S., Wells, N., Hicks, J., Larson, S.A., Wiedermann, J.P., Carver, K., et al. (2008). Genetic differences in human circadian clock genes among worldwide populations. J. Biol. Rhythms *23*, 330–340.

Cingolani, P., Platts, A., Wang, Le, L., Coon, M., Nguyen, T., Wang, L., Land, S.J., Lu, X., and Ruden, D.M. (2012). A program for annotating and predicting the effects of single nucleotide polymorphisms, SnpEff: SNPs in the genome of Drosophila melanogaster strain w1118; iso-2; iso-3. Fly (Austin) *6*, 80–92.

Crane, B.R., and Young, M.W. (2014). Interactive features of proteins composing eukaryotic circadian clocks. Annu. Rev. Biochem. *83*, 191–219.

Czarna, A., Breitkreuz, H., Mahrenholz, C.C., Arens, J., Strauss, H.M., and Wolf, E. (2011). Quantitative analyses of cryptochrome-mBMAL1 interactions: mechanistic insights into the transcriptional regulation of the mammalian circadian clock. J. Biol. Chem. *286*, 22414–22425.

Czeisler, C.A., Duffy, J.F., Shanahan, T.L., Brown, E.N., Mitchell, J.F., Rimmer, D.W., Ronda, J.M., Silva, E.J., Allan, J.S., Emens, J.S., et al. (1999). Stability, precision, and near-24-hour period of the human circadian pacemaker. Science *284*, 2177–2181.

Danecek, P., Auton, A., Abecasis, G., Albers, C.A., Banks, E., DePristo, M.A., Handsaker, R.E., Lunter, G., Marth, G.T., Sherry, S.T., et al.; 1000 Genomes Project Analysis Group (2011). The variant call format and VCFtools. Bioinformatics *27*, 2156–2158.

DePristo, M.A., Banks, E., Poplin, R., Garimella, K.V., Maguire, J.R., Hartl, C., Philippakis, A.A., del Angel, G., Rivas, M.A., Hanna, M., et al. (2011). A framework for variation discovery and genotyping using next-generation DNA sequencing data. Nat. Genet. *43*, 491–498.

Duffy, J.F., Rimmer, D.W., and Czeisler, C.A. (2001). Association of intrinsic circadian period with morningness-eveningness, usual wake time, and circadian phase. Behav. Neurosci. *115*, 895–899.

Duong, H.A., Robles, M.S., Knutti, D., and Weitz, C.J. (2011). A molecular mechanism for circadian clock negative feedback. Science *332*, 1436–1439.

Duong, H.A., and Weitz, C.J. (2014). Temporal orchestration of repressive chromatin modifiers by circadian clock Period complexes. Nat. Struct. Mol. Biol. *21*, 126–132.

Ebisawa, T., Uchiyama, M., Kajimura, N., Mishima, K., Kamei, Y., Katoh, M., Watanabe, T., Sekimoto, M., Shibui, K., Kim, K., et al. (2001). Association of structural polymorphisms in the human period3 gene with delayed sleep phase syndrome. EMBO Rep. *2*, 342–346.

Gao, P., Yoo, S.H., Lee, K.J., Rosensweig, C., Takahashi, J.S., Chen, B.P., and Green, C.B. (2013). Phosphorylation of the cryptochrome 1 C-terminal tail regulates circadian period length. J. Biol. Chem. *288*, 35277–35286.

Godinho, S.I., Maywood, E.S., Shaw, L., Tucci, V., Barnard, A.R., Busino, L., Pagano, M., Kendall, R., Quwailid, M.M., Romero, M.R., et al. (2007). The after-hours mutant reveals a role for Fbxl3 in determining mammalian circadian period. Science *316*, 897–900.

Griffin, E.A., Jr., Staknis, D., and Weitz, C.J. (1999). Light-independent role of CRY1 and CRY2 in the mammalian circadian clock. Science *286*, 768–771.

Gronfier, C., Wright, K.P., Jr., Kronauer, R.E., and Czeisler, C.A. (2007). Entrainment of the human circadian pacemaker to longer-than-24-h days. Proc. Natl. Acad. Sci. USA *104*, 9081–9086.

Hawkins, G.A., Meyers, D.A., Bleecker, E.R., and Pack, A.I. (2008). Identification of coding polymorphisms in human circadian rhythm genes PER1, PER2, PER3, CLOCK, ARNTL, CRY1, CRY2 and TIMELESS in a multi-ethnic screening panel. DNA Seq. *19*, 44–49.

Hida, A., Kitamura, S., Katayose, Y., Kato, M., Ono, H., Kadotani, H., Uchiyama, M., Ebisawa, T., Inoue, Y., Kamei, Y., et al. (2014). Screening of clock gene polymorphisms demonstrates association of a PER3 polymorphism with morningness-eveningness preference and circadian rhythm sleep disorder. Sci. Rep. *4*, 6309.

Hirano, A., Shi, G., Jones, C.R., Lipzen, A., Pennacchio, L.A., Xu, Y., Hallows, W.C., McMahon, T., Yamazaki, M., Ptáček, L.J., and Fu, Y.H. (2016). A Cryptochrome 2 mutation yields advanced sleep phase in humans. eLife *5*, e16695.

Hirayama, J., Sahar, S., Grimaldi, B., Tamaru, T., Takamatsu, K., Nakahata, Y., and Sassone-Corsi, P. (2007). CLOCK-mediated acetylation of BMAL1 controls circadian function. Nature *450*, 1086–1090.

Hirota, T., Lee, J.W., St John, P.C., Sawa, M., Iwaisako, K., Noguchi, T., Pongsawakul, P.Y., Sonntag, T., Welsh, D.K., Brenner, D.A., et al. (2012). Identification of small molecule activators of cryptochrome. Science *337*, 1094–1097.

Hur, Y.M., Bouchard, T.J., and Lykken, D.T. (1998). Genetic and environmental influence on morningness–eveningness. Pers. Individ. Dif. *25*, 917–925.

Khan, S.K., Xu, H., Ukai-Tadenuma, M., Burton, B., Wang, Y., Ueda, H.R., and Liu, A.C. (2012). Identification of a novel cryptochrome differentiating domain required for feedback repression in circadian clock function. J. Biol. Chem. *287*, 25917–25926.

King, D.P., Zhao, Y., Sangoram, A.M., Wilsbacher, L.D., Tanaka, M., Antoch, M.P., Steeves, T.D., Vitaterna, M.H., Kornhauser, J.M., Lowrey, P.L., et al. (1997). Positional cloning of the mouse circadian clock gene. Cell *89*, 641–653.

Koskenvuo, M., Hublin, C., Partinen, M., Heikkilä, K., and Kaprio, J. (2007). Heritability of diurnal type: a nationwide study of 8753 adult twin pairs. J. Sleep Res. *16*, 156–162.

Kripke, D.F., Klimecki, W.T., Nievergelt, C.M., Rex, K.M., Murray, S.S., Shekhtman, T., Tranah, G.J., Loving, R.T., Lee, H.J., Rhee, M.K., et al. (2014). Circadian polymorphisms in night owls, in bipolars, and in non-24-hour sleep cycles. Psychiatry Investig. *11*, 345–362.

Kume, K., Zylka, M.J., Sriram, S., Shearman, L.P., Weaver, D.R., Jin, X., Maywood, E.S., Hastings, M.H., and Reppert, S.M. (1999). mCRY1 and mCRY2 are essential components of the negative limb of the circadian clock feedback loop. Cell *98*, 193–205.

Lek, M., Karczewski, K.J., Minikel, E.V., Samocha, K.E., Banks, E., Fennell, T., O'Donnell-Luria, A.H., Ware, J.S., Hill, A.J., Cummings, B.B., et al.; Exome Aggregation Consortium (2016). Analysis of protein-coding genetic variation in 60,706 humans. Nature *536*, 285–291.

Li, H., and Durbin, R. (2009). Fast and accurate short read alignment with Burrows-Wheeler transform. Bioinformatics *25*, 1754–1760.

Li, Y., Xiong, W., and Zhang, E.E. (2016). The ratio of intracellular CRY proteins determines the clock period length. Biochem. Biophys. Res. Commun. *472*, 531–538.

Liu, A.C., Tran, H.G., Zhang, E.E., Priest, A.A., Welsh, D.K., and Kay, S.A. (2008). Redundant function of REV-ERBalpha and beta and non-essential role for Bmal1 cycling in transcriptional regulation of intracellular circadian rhythms. PLoS Genet. *4*, e1000023.

Lowrey, P.L., and Takahashi, J.S. (2011). Genetics of circadian rhythms in Mammalian model organisms. Adv. Genet. *74*, 175–230.

McLaren, W., Gil, L., Hunt, S.E., Riat, H.S., Ritchie, G.R., Thormann, A., Flicek, P., and Cunningham, F. (2016). The Ensembl Variant Effect Predictor. Genome Biol. *17*, 122.

Menet, J.S., Abruzzi, K.C., Desrochers, J., Rodriguez, J., and Rosbash, M. (2010). Dynamic PER repression mechanisms in the Drosophila circadian clock: from on-DNA to off-DNA. Genes Dev. *24*, 358–367.

Merbitz-Zahradnik, T., and Wolf, E. (2015). How is the inner circadian clock controlled by interactive clock proteins?: Structural analysis of clock proteins elucidates their physiological role. FEBS Lett. *589*, 1516–1529.

Micic, G., de Bruyn, A., Lovato, N., Wright, H., Gradisar, M., Ferguson, S., Burgess, H.J., and Lack, L. (2013). The endogenous circadian temperature period length (tau) in delayed sleep phase disorder compared to good sleepers. J. Sleep Res. *22*, 617–624.

Molina, T.A., and Burgess, H.J. (2011). Calculating the dim light melatonin onset: the impact of threshold and sampling rate. Chronobiol. Int. *28*, 714–718.

Ode, K.L., Ukai, H., Susaki, E.A., Narumi, R., Matsumoto, K., Hara, J., Koide, N., Abe, T., Kanemaki, M.T., Kiyonari, H., et al. (2016). Knockout-rescue embryonic stem cell-derived mouse reveals circadian-period control by quality and quantity of CRY1. Mol. Cell *65*, 176–190.

Oshima, T., Yamanaka, I., Kumar, A., Yamaguchi, J., Nishiwaki-Ohkawa, T., Muto, K., Kawamura, R., Hirota, T., Yagita, K., Irle, S., et al. (2015). C-H activation generates period-shortening molecules that target cryptochrome in the mammalian circadian clock. Angew. Chem. Int. Ed. Engl. *54*, 7193–7197.

Osland, T.M., Bjorvatn, B.R., Steen, V.M., and Pallesen, Sl. (2011). Association study of a variable-number tandem repeat polymorphism in the clock gene PERIOD3 and chronotype in Norwegian university students. Chronobiol. Int. *28*, 764–770.

Oster, H., Yasui, A., van der Horst, G.T., and Albrecht, U. (2002). Disruption of mCry2 restores circadian rhythmicity in mPer2 mutant mice. Genes Dev. *16*, 2633–2638.

Özçelik, T., and Onat, O.E. (2016). Genomic landscape of the Greater Middle East. Nat. Genet. *48*, 978–979.

Pereira, D.S., Tufik, S., Louzada, F.M., Benedito-Silva, A.A., Lopez, A.R., Lemos, N.A., Korczak, A.L., D'Almeida, V., and Pedrazzoli, M. (2005). Association of the length polymorphism in the human Per3 gene with the delayed sleep-phase syndrome: does latitude have an influence upon it? Sleep *28*, 29–32.

Pittendrigh, C.S., and Daan, S. (1976). Functional-Analysis of Circadian Pacemakers in Nocturnal Rodents 0.1. Stability and Lability of Spontaneous Frequency. J. Comp. Physiol. *106*, 223–252.

Preitner, N., Damiola, F., Lopez-Molina, L., Zakany, J., Duboule, D., Albrecht, U., and Schibler, U. (2002). The orphan nuclear receptor REV-ERBalpha controls circadian transcription within the positive limb of the mammalian circadian oscillator. Cell *110*, 251–260.

Roenneberg, T., Wirz-Justice, A., and Merrow, M. (2003). Life between clocks: daily temporal patterns of human chronotypes. J. Biol. Rhythms *18*, 80–90.

Sack, R.L., Auckley, D., Auger, R.R., Carskadon, M.A., Wright, K.P., Jr., Vitiello, M.V., and Zhdanova, I.V.; American Academy of Sleep Medicine (2007). Circadian rhythm sleep disorders: part II, advanced sleep phase disorder, delayed sleep phase disorder, free-running disorder, and irregular sleep-wake rhythm. An American Academy of Sleep Medicine review. Sleep *30*, 1484–1501.

Shimomura, K., Kumar, V., Koike, N., Kim, T.K., Chong, J., Buhr, E.D., Whiteley, A.R., Low, S.S., Omura, C., Fenner, D., et al. (2013). Usf1, a suppressor of the circadian Clock mutant, reveals the nature of the DNA-binding of the CLOCK:BMAL1 complex in mice. eLife *2*, e00426.

Siepka, S.M., Yoo, S.H., Park, J., Song, W., Kumar, V., Hu, Y., Lee, C., and Takahashi, J.S. (2007). Circadian mutant Overtime reveals F-box protein FBXL3 regulation of cryptochrome and period gene expression. Cell *129*, 1011–1023.

Toh, K.L., Jones, C.R., He, Y., Eide, E.J., Hinz, W.A., Virshup, D.M., Ptácek, L.J., and Fu, Y.H. (2001). An hPer2 phosphorylation site mutation in familial advanced sleep phase syndrome. Science *291*, 1040–1043.

Ueda, H.R., Chen, W., Adachi, A., Wakamatsu, H., Hayashi, S., Takasugi, T., Nagano, M., Nakahama, K., Suzuki, Y., Sugano, S., et al. (2002). A transcription factor response element for gene expression during circadian night. Nature *418*, 534–539.

Ukai-Tadenuma, M., Yamada, R.G., Xu, H., Ripperger, J.A., Liu, A.C., and Ueda, H.R. (2011). Delay in feedback repression by cryptochrome 1 is required for circadian clock function. Cell *144*, 268–281.

van der Horst, G.T., Muijtjens, M., Kobayashi, K., Takano, R., Kanno, S., Takao, M., de Wit, J., Verkerk, A., Eker, A.P., van Leenen, D., et al. (1999). Mammalian Cry1 and Cry2 are essential for maintenance of circadian rhythms. Nature *398*, 627–630.

Vink, J.M., Groot, A.S., Kerkhof, G.A., and Boomsma, D.I. (2001). Genetic analysis of morningness and eveningness. Chronobiol. Int. *18*, 809–822.

Vitaterna, M.H., Selby, C.P., Todo, T., Niwa, H., Thompson, C., Fruechte, E.M., Hitomi, K., Thresher, R.J., Ishikawa, T., Miyazaki, J., et al. (1999). Differential regulation of mammalian period genes and circadian rhythmicity by cryptochromes 1 and 2. Proc. Natl. Acad. Sci. USA *96*, 12114–12119.

Weitzman, E.D., Czeisler, C.A., Coleman, R.M., Spielman, A.J., Zimmerman, J.C., Dement, W., Richardson, G., and Pollak, C.P. (1981). Delayed sleep phase syndrome. A chronobiological disorder with sleep-onset insomnia. Arch. Gen. Psychiatry *38*, 737–746.

Wright, K.P., Jr., Gronfier, C., Duffy, J.F., and Czeisler, C.A. (2005). Intrinsic period and light intensity determine the phase relationship between melatonin and sleep in humans. J. Biol. Rhythms *20*, 168–177.

Xu, H., Gustafson, C.L., Sammons, P.J., Khan, S.K., Parsley, N.C., Ramanathan, C., Lee, H.W., Liu, A.C., and Partch, C.L. (2015). Cryptochrome 1 regulates the circadian clock through dynamic interactions with the BMAL1 C terminus. Nat. Struct. Mol. Biol. *22*, 476–484.

Xu, Y., Padiath, Q.S., Shapiro, R.E., Jones, C.R., Wu, S.C., Saigoh, N., Saigoh, K., Ptácek, L.J., and Fu, Y.H. (2005). Functional consequences of a CKIdelta mutation causing familial advanced sleep phase syndrome. Nature *434*, 640–644.

Xu, Y., Toh, K.L., Jones, C.R., Shin, J.Y., Fu, Y.H., and Ptácek, L.J. (2007). Modeling of a human circadian mutation yields insights into clock regulation by PER2. Cell *128*, 59–70.

Ye, R., Selby, C.P., Chiou, Y.Y., Ozkan-Dagliyan, I., Gaddameedhi, S., and Sancar, A. (2014). Dual modes of CLOCK:BMAL1 inhibition mediated by Cryptochrome and Period proteins in the mammalian circadian clock. Genes Dev. *28*, 1989–1998.

Zee, P.C., Attarian, H., and Videnovic, A. (2013). Circadian rhythm abnormalities. Continuum (Minneap. Minn.) *19*(1 Sleep Disorders), 132–147.

Zhang, E.E., Liu, A.C., Hirota, T., Miraglia, L.J., Welch, G., Pongsawakul, P.Y., Liu, X., Atwood, A., Huss, J.W., 3rd, Janes, J., et al. (2009). A genome-wide RNAi screen for modifiers of the circadian clock in human cells. Cell *139*, 199–210.

STAR★METHODS

KEY RESOURCES TABLE

REAGENT or RESOURCE	SOURCE	IDENTIFIER
Antibodies		
Rabbit polyclonal anti-Cry1	Bethyl Laboratories	Cat# A302-614A; RRID: AB_10555376
Rabbit polyclonal anti-Bmal1	Bethyl Laboratories	Cat# A302-616A; RRID: AB_10555918
Rabbit polyclonal anti-Clock	Bethyl Laboratories	Cat# A302-618A; RRID: AB_10555233
Rabbit polyclonal anti-NFX1	Bethyl Laboratories	Cat# A302-914A; RRID: AB_10663488
Rabbit polyclonal anti-Per2	Alpha Diagnostics	Cat# PER21-A
Rabbit polyclonal anti-acetyl BMAL1 (Lys538)	Millipore	Cat# AB15396; RRID: AB_11212017
Rabbit monoclonal anti-Trimethyl-Histone H3 (Lys4)	Millipore	Cat# 17-614; RRID: AB_11212770
Mouse monoclonal anti-α-Tubulin clone DM1A	Sigma	Cat# T6199; RRID: AB_477583
Mouse monoclonal anti-TATA binding protein TBP	Abcam	Cat# 51841; RRID: AB_945758
Chemicals, Peptides, and Recombinant Proteins		
Forskolin	Sigma-Aldrich	Cat# F3917
D-Luciferin Firefly, Potassium salt	Biosynth	Cat# L-8220
Critical Commercial Assays		
Bühlmann Direct Saliva Melatonin Radio Immunoassay kit	ALPCO Diagnostics	Cat# 01-RK-DSM2
Oragene DNA Self-Collection kit	DNA Genotek	Cat# OG-500
Dual-Luciferase Reporter Assay System	Promega	Cat# E1910
Agilent SureSelect Human All Exon V4 capture kit	Agilent Technologies	Design ID: S03723314
Deposited Data		
GRCh37	1000 Genomes	http://www.internationalgenome.org/
Human subject details	This study	Table S1
Experimental Models: Cell Lines		
Primary human dermal fibroblasts	This study	N/A
Cry-deficient mouse embryonic fibroblasts	Ukai-Tadenuma et al., 2011	N/A
HEK293T/17	ATCC	Cat# CRL-11268
Recombinant DNA		
pLenti6-Bmal1-dLuc	Liu et al., 2008	N/A
psPax2	Addgene	Cat# 12260
pMD2G	Addgene	Cat# 12259
pLV6puro-hCry1fl	This study	N/A
pLV6puro-hCry1Δ	This study	N/A
pLV6puro-promoter	This study	N/A
pcDNA3HA-hCry1fl	This study	N/A
pcDNA3HA-hCry1fl	This study	N/A
pcDNA3F-hBmal1	This study	N/A
pcDNA3F-hClock	This study	N/A
pGL3-AVP	Kume et al., 1999	N/A
pGL3-Per2dLuc	Ueda et al., 2002	N/A
pcDNA3F-hCry1fl-luc	This study	N/A
pcDNA3F-hCry1Δ-luc	This study	N/A
Sequence-Based Reagents		
Primers for RT-PCR, see Table S3		

(*Continued on next page*)

Continued

REAGENT or RESOURCE	SOURCE	IDENTIFIER
Primers for ChIP, see Table S3		
Primers for genotyping, see Table S3		
Software and Algorithms		
PSG TWin (version 4.1.)	Grass Technologies, Natus Neurology	http://www.natus.com/
ClockLab (version 2.72)	Actimetrics	http://actimetrics.com/downloads/clocklab/
Lumicycle (version 2.54)	Actimetrics	http://actimetrics.com/downloads/lumicycle/
Prism (version 5.0c)	GraphPad Software	https://www.graphpad.com/scientific-software/prism/
ImageJ (version 1.49v)	NIH	https://imagej.nih.gov/ij
Burrows-Wheeler Aligner (BWA version 0.7.8)	Li and Durbin, 2009	http://bio-bwa.sourceforge.net/
Picard (version 1.83)	Broad Institute	https://broadinstitute.github.io/picard/
GATK (Genome Analysis Toolkit version 3.2-2)	DePristo et al., 2011	http://gatkforums.broadinstitute.org/gatk
SnpEff (version 3.4b)	Cingolani et al., 2012	http://snpeff.sourceforge.net/
VCFtools (version 0.1.11)	Danecek et al., 2011	https://vcftools.github.io/index.html
Ensembl Variant Effect Predictor	McLaren et al., 2016	http://grch37.ensembl.org/Homo_sapiens/Tools/VEP
Other		
Aura PSG Lite portable polysomnography system	Grass Technologies, Natus Neurology	http://www.natus.com/
VitalSense telemetric core body temperature monitoring system	Philips Respironics	http://www.actigraphy.com/solutions/vitalsense/
Actiwatch activity monitoring system	Philips Respironics	http://www.actigraphy.com/solutions/actigraphy.html

CONTACT FOR REAGENT AND RESOURCE SHARING

For reagents generated in this study or any other questions about the reagents please contact the Lead Contact Michael W. Young (young@rockefeller.edu).

EXPERIMENTAL MODEL AND SUBJECT DETAILS

Human Studies

Human subject research was approved by Institutional Review Boards at Weill Cornell Medical College (WCMC protocol 0609008750) and The Rockefeller University (RU protocol APA-0777) and the ethics committee at Bilkent University. Subjects' written informed consent was obtained prior to any study procedures. Subject details can be found in Table S1.

Subject Screening for Human In-Laboratory Study

Sleep behavior was assessed through sleep interview, sleep and chronotype questionnaires and at-home actigraphy (Actiwatch-L, Philips Respironics) combined with a sleep log prior to arrival at the laboratory. Eligibility required habitual bedtimes between 22:30 – 00:30 with habitual waketimes between 06:00 – 09:00 for controls and habitual bedtimes later than 02:00 with habitual waketimes later than 10:00 for DSPD subjects. Subjects were confirmed to be in good physical and mental health at the time of study participation based on physical exam, urine toxicology screen, structured diagnostic interview (SCID-R) and Hamilton Depression Rating Scale.

Data Collection for Human In-Laboratory Study

Subjects resided in a research studio apartment, which was located within the WCMC Laboratory of Human Chronobiology and shielded from all cues to time-of-day. Closed-circuit TV allowed for observation of subjects and communication was possible through an intercom system. Laboratory personnel also intermittently entered the research apartment for in-person interaction as necessary. Illumination was limited to a maximum of 100 lux with average values between 30 and 50 lux, except during sample collection for salivary DLMO when maximum illumination at the eye level when subjects were seated was set to 16 lux. Continuous electroencephalogram (EEG), electrooculogram (EOG) and electromyogram (EMG) were recorded using a portable polysomnography (PSG) system (Aura PSG Lite, Grass Technologies, Natus Neurology, West Warwick, RI) and a PSG electrode montage consisting of 6 referential EEG derivations referenced to linked mastoids. Core body temperature was recorded in 1 min intervals using ingestible telemetric temperature sensors with an external wireless data receiver (VitalSense, Philips Respironics). Saliva samples for DLMO

determination were collected in 30 min intervals on the evening leading up to the second entrainment night starting at 18:00 until bedtime. Subjects were instructed to sit quietly and refrain from eating or drinking prior to each sample collection. Samples were collected using Salivette tubes (ALPCO Diagnostics, Windham NH) and stored frozen until analysis by the Yerkes Endocrine Assay Laboratory of Emory University using the Bühlmann Direct Saliva Melatonin Radio Immunoassay kit (ALPCO Diagnostics, Windham NH). A fixed threshold of 3 pg/ml was used for DLMO estimation (Benloucif et al., 2008).

Proband Family Study

Sleep behavior was assessed by sleep and chronotype questionnaires and sleep interview (in-person or via phone). Select subjects also complied with a request to maintain a sleep log for 14 days (see Figure S2). Genomic DNA was isolated from saliva (Oragene DNA Self-Collection kit, DNA genotek) and, additionally for select subjects, whole blood (BD Vacutainer K2 EDTA) using the Gentra Puregene Blood Kit (QIAGEN).

Reverse Phenotyping of additional CRY1 c.1657+3A>C Carrier Families

Carriers of the CRY1 c.1657+3A>C allele were identified from an in-house exome database of families with metabolic and neurodegenerative phenotypes at Bilkent University and from databases maintained by the University and Scientific and Technological Research Council of Turkey, Advanced Genomics and Bioinformatics Research Center (TÜBİTAK-IGBAM, http://www.igbam.bilgem.tubitak.gov.tr/en/index.html). Neither of these databases is publicly accessible. Requests for materials, data, and further information should be addressed to Tayfun Ozcelik (tozcelik@bilkent.edu.tr, see also Data And Software Availability). Ethics and consent procedures for subjects in these databases allow for re-contact. Upon outreach from Bilkent University investigators, subjects in seven families (DSPD-1, −2, −4, −6, −7, −9 and −14) consented to characterization of their sleep behavior and donation of a DNA sample for genotyping. Habitual sleep times were determined from questionnaires and factors that could potentially confound sleep characterization were assessed through interview (in-person or via phone). The latter included any relevant comorbidities and medications as well as environmental factors such as current or former shift work, religious observances (5 am prayer) and family circumstances (influence of spouse on bed and wake times, number of young children, pregnancy). One family DSPD-2 was excluded from further analysis after data collection because of complete co-segregation of aberrant sleep in carriers with morbid obesity and obstructive sleep apnea. For the remaining families, subjects were classified into the following categories: affected late, affected fragmented, probably affected, probably not affected, not affected or uninterpretable. Factors that contributed to the classification of each subject are listed in Table S1. For the statistical analysis of the association of sleep behavior with *CRY1* allele status, the first three categories were combined as 'affected' and the third and fourth category were combined as 'unaffected'. P value from Fisher's exact test, odds ratio and 95% confidence interval were calculated in Prism 5 (GraphPad Software). Note: The term carrier is used in this work in reference to individuals who carry one or two copies of the dominant CRY1 c.1657+3A>C allele, analogous to common practice in clinical settings for disease-linked dominant genetic variants. This nomenclature should not to be confused with the classical genetic definition of a carrier as an individual carrying a recessive allele who is unaffected by the trait.

Derivation of Human Dermal Fibroblast Cell Lines

A 4 mm full thickness skin punch biopsy was taken from a subject's thigh under local anesthesia and immediately transferred to a vial containing sterile storage medium (DMEM with 50% fetal bovine serum (FBS)). Tissue processing for establishment of dermal fibroblast cell lines was performed within the next several hours using the following procedure modified from Brown et al. (Brown et al., 2005). Briefly, samples were digested overnight in primary culture medium (DMEM containing 20% FBS, antibiotics (100 U/ml penicillin and 100 μg/ml streptomycin (GIBCO, Life Technologies)), 2.5 μg/ml Amphotericin B (Sigma)) supplemented with 100 μg/ml Collagenase Type I (GIBCO, Life Technologies) and 100 μg/ml Dispase (GIBCO, Life Technologies). Cells were cultured in primary culture medium until the first passage when the FBS concentration was reduced to 10% and Amphotericin B was omitted from the culture medium.

Cell Lines and Tissue Culture

Primary dermal fibroblast cell lines were derived from a subject's skin punch biopsy as described above. 293T cells were obtained from ATCC. Cry1/2 double knockout mouse embryonic fibroblasts (DKO MEFs) have been described (Ukai-Tadenuma et al., 2011). Cells were maintained in standard culture medium DMEM (Invitrogen, Life Technologies) with antibiotics (100 U/ml penicillin and 100 μg/ml streptomycin (GIBCO, Life Technologies)) and fetal bovine serum (10% FBS for dermal fibroblasts and 293T cells, 2% FBS for DKO MEFs). For clock synchronization, cells were treated with 20 μM forskolin (Sigma) in culture medium for 1.5 hr. Lentivirus was prepared by transient transfection of 293T cells with second generation lentiviral vectors using standard calcium phosphate transfection methods. Filtered, unconcentrated supernatant with 8 μg/ml polybrene (Millipore) was used for transduction. Selection antibiotic (10 μg/ml blasticidin or 2.5 μg/ml puromycin, both Invivogen) was added to cell culture medium three days post-transduction.

METHOD DETAILS

Candidate Gene Sequencing

cDNAs for the below listed clock genes were cloned from total RNA isolated from the proband TAU11 dermal fibroblast cell line and sequenced by Sanger sequencing. In addition to the CRY1 c.1657+3A>C variant, the following coding variations were identified (variants are listed with dbSNP identifier and alternate allele frequency):

PER1 (GenBank: NM_002616.2, NP_002607.2)		
c.2884G>C (p.Ala962Pro)	rs2585405	AF 1-0.2282
c.2992G>A (p.Ala998Thr)	rs112474322	AF 0.0154
PER2 (GenBank: NM_022817.2, NP_073728.1)		
c.1201C>T (p.Arg401Cys)	rs77146655	AF 0.0106
PER3 (GenBank: NM_016831.2, 058515.1)		
c.1916T>G (p.Val639Gly)	rs10462020	AF 0.1206
c.2480T>C (p.Leu827Pro)	rs228696	AF 1-0.0248
c.3083T>C (p.Met1028Thr)	rs2640909	AF 0.1853
c.3446A>C (p.His1149Arg)	rs10462021	AF 0.1210
CRY1: no additional coding change		
CRY2, ARNTL, CLOCK, CSNK1D: no coding change		

The presence of additional polymorphisms is not unexpected given the large degree of variation commonly found in some human clock genes (Ciarleglio et al., 2008; Hawkins et al., 2008). The *PER1* polymorphisms were not considered likely DPSD alleles based on high allele frequency and their presence in control subjects of normal chronotype. Regarding the *PER2* variant, the arginine to cysteine amino acid change appears to constitute a reversion to the ancestral allele based on the fact that this position encodes a cysteine in both human PER1 and PER3 as well as in many vertebrate members of the Per2 family with the exception of placental mammals. Although a functional effect of this amino acid change is thus unlikely, we assessed its segregation with aberrant sleep in the proband kindred. Based on absence of the *PER2* allele in the proband's affected mother TAUX01 and nieces TAUX08 and TAUX10, the variant was disregarded as a potential DSPD allele. Although several coding variations in *PER3* have been associated with late chronotype and DPSD behavior (Archer et al., 2003; Ebisawa et al., 2001; Hida et al., 2014), subsequent studies have often struggled to reproduce these findings, possibly due to limited sample and effect sizes or population-specific correlations in the original studies (Kripke et al., 2014; Osland et al., 2011; Pereira et al., 2005). Among the proposed *PER3* polymorphisms, the Val639Gly allele was detected in the TAU11 proband as well as several of our other subjects (both DSPD and normal chronotype controls). Although the fact that this allele is not uncommon in normal controls argues against a causal role of the variant in delayed sleep behavior, we assessed its segregation with aberrant sleep patterns in the proband kindred. We found the alternate allele to be very common in both heterozygous and homozygous forms throughout the family albeit with poor behavioral correlation (e.g., unaffected cousin TAUX04 is homozygous carrier, whereas affected niece TAUX10 lacks alternate Gly allele). Although it remains possible that the presence of this allele may influence chronotype preference in conjunction with additional genetic or environmental factors yet to be characterized, these results do not support a causal role of this variant in sleep behavior in the proband kindred.

Whole Exome Sequencing

Genomic DNA was isolated from the proband fibroblast cell line or whole blood samples from subjects TAUX01-04 using the Gentra Puregene Blood Kit (QIAGEN). Whole exome sequencing (WES) was performed by the New York Genome Center as follows: Exome capture was performed using Agilent SureSelect Human All Exon V4 capture kit. 100 bp paired-end sequencing was done on Illumina HiSeq 2500. Sequences were aligned to human genome build GRCh37 using BWA (Burrows-Wheeler Aligner) (Li and Durbin, 2009). Duplicate reads were marked using Picard (http://picard.sourceforge.net). GATK (Genome Analysis Toolkit) (DePristo et al., 2011) was used for base quality score recalibration (BQSR) and local realignment around indels to refine alignment artifacts around putative insertions or deletions. Variant discovery was performed in two steps - variant calling with GATK HaplotypeCaller followed by joint genotyping using GATK GenotypeGVCFs. The resulting variant call set was refined using Variant Quality Score Recalibration (VQSR) as implemented in GATK VariantRecalibrator. The VQSR scores were used to define low quality variants for downstream processing. SnpEff (Cingolani et al., 2012) and VCFtools (Danecek et al., 2011) were used to add variant effect predictions and functional annotations.

WES of the proband TAU11 confirmed all previously identified variants, but did not identify any additional coding variations in the above studied clock genes or additional candidate genes *CSNK1E*, *ARNTL2*, *FBXL3*, *FBXL21*, *BHLHE40*, *BHLHE41*, *NR1D1* and *RORA*. A single coding variation was detected in TIMELESS c.2492G>A (p.Arg831Gln), which was not considered further based on high allele frequency in the general population (AF 0.4988, rs774047).

WES of four affected family members (TAU11, TAUX01, TAUX02, TAUX03) and one unaffected family member (TAUX4) of the proband's family was carried out in order to identify all potentially functional genetic variants co-segregating with the sleep phenotype. Variants were annotated, then filtered as follows: (1) to include only variants with minor allele frequencies < 0.01 in the 1000 Genomes combined population using Ensembl Variant Effect Predictor (McLaren et al., 2016) or in the ExAC total population (Lek et al., 2016); (2) to include only variants at a site with gerp score > 2.0 or a nonsynonymous change with PolyPhen score > 0.40 (PolyPhen-2 v2.2.2r398); and (3) to include only variants shared by all affected family members and not present in the unaffected family member. Among the remaining variants (Table S2), the CRY1 c.1657+3A>C allele was the only variant affecting a gene with a known or implicated role in the regulation of sleep or circadian rhythmicity.

Of the additional clock gene coding variations found in the proband TAU11 (see above), none segregated with sleep behavior in the additional exome-sequenced subjects:

	TAUX01 (affected)	TAUX02 (affected)	TAUX03 (affected)	TAUX04 (not affected)
rs2585405	present	present	present	present
rs112474322	not present	not present	present	not present
rs77146655	not present	present	present	not present
rs10462020	present	present	present	present
rs228696	present	present	present	present
rs2640909	present	present	present	present
rs10462021	present	present	present	present

CRY1 c.1657+3A>C Genotyping

For *CRY1* genotyping, a 623 base pair fragment of the genomic locus containing exon 11 was PCR amplified using oligos hCry1i10F and hCry1i12R (Table S3). The product was either Sanger-sequenced or tested for a restriction fragment length polymorphism for Hpy188I (+ allele: no cut, variant c.1657+3A>C: 276 bp + 347 bp).

Cloning of *CRY1* Constructs

Human *CRY1* full-length (fl) and Δ11 cDNAs were PCR amplified from a first-strand cDNA library from the proband fibroblast cell line and blunt-cloned into the EcoRV-site of pBluescript. Sequences were confirmed by Sanger-sequencing. Aside from the 72 base pairs missing in Δ11, sequences were identical to Refseq human *CRY1* (GenBank: NM_004075.4) with the exception of a common silent variant c.636T>C (p.Gly212=, rs8192440, AF 1-0.2103) present in both *CRY1* forms. ORFs were subcloned in frame into a modified pcDNA3.1 vector (Invitrogen, Life Technologies) containing an N-terminal triple-HA tag using EcoRV/NotI restriction sites. For lentiviral expression, *CRY1* fl and Δ11 were PCR-amplified and first subcloned into pMU2-P(Cry1)-(Cry1 intron336)-Cry1 (Ukai-Tadenuma et al., 2011) from which the *mCry1* cDNA had been excised using XbaI/NotI restriction sites, yielding pMU2-hCry1fl and Δ11. The *mCry1* expression cassette of pMU2-P(Cry1)-(Cry1 intron336)-Cry1, including promoter, intronic sequence and *mCry1* cDNA was transferred into a modified pLenti6 vector (Invitrogen, Life Technologies), in which the blasticidin resistence cassette had been replaced with puromycin using SalI/MluI restriction sites, yielding pLV6puro-mCry1. To generate pLV6puro-hCry1fl and Δ11, *mCry1* in pLV6puro-mCry1 was replaced with *CRY1* cDNAs amplified from pMU2-hCry1 constructs using XbaI/MluI restriction sites. To generate an 'empty vector' control containing only the *Cry1* regulatory elements without cDNA, the XbaI/MluI-digested vector was blunted with T4 DNA polymerase and religated.

Real-Time Circadian Reporter Assay

Cry DKO MEFs were transduced with a lentiviral Bmal-luc reporter (Liu et al., 2008) and with lentiviral *CRY1* fl or Δ11 (pLV6puro-hCry1fl and Δ11) and selected for transgene expression using appropriate selection antibiotics. Cells were plated and grown to confluence in 35 mm dishes (BD Falcon) and synchronized with 20 μg/ml forskolin (Sigma) for 1.5 hr. Medium was replaced with counting medium (phenol red-, L-glutamine- and bicarbonate-free DMEM (Cellgro), 100 U/ml penicillin and 100 μg/ml streptomycin, 2% FBS, 350 mg/l sodium bicarbonate (GIBCO), 10 mM HEPES pH 7.2 (GIBCO), 2 mM L-glutamine (GIBCO), 0.5 mM firefly D-luciferin potassium salt (Biosynth)) and dishes were sealed with high vacuum grease (Dow Corning). Bioluminescence was recorded for approximately seven days in a Lumicycle luminometer (Actimetrics) with counts collected in 10 min intervals for each dish. The first ~20 hr of recorded data were excluded from analysis. Period analysis was performed by fitting a damped sine curve to time series data detrended by subtracting a running average using Lumicycle analysis software (Actimetrics). Goodness-of-fit values for curve fitting were routinely above 90%. Statistical significance between genotypes was assessed using an unpaired t test.

Preparation of Protein Extracts, Immunoprecipitation, and Western Blot

For subcellular fractionation, cells were first lysed in buffer 1 containing 320 mM sucrose, 10 mM Tris-HCl pH 8.0, 3 mM $CaCl_2$, 2 mM Mg Acetate, 0.1 mM EDTA, 0.05% Triton X-100 and freshly added 1 mM DTT, protease inhibitor cocktail (Sigma) and phosphatase

inhibitor cocktails (Sigma). Nuclei were collected by centrifugation and the supernatant saved as the cytoplasmic fraction. Nuclei were washed in buffer 2 (buffer 1 lacking detergent) and lysed as follows: Nuclear extracts for Western Blot were prepared in buffer 3 (500 mM NaCl, 50 mM Tris-HCl pH 8.0, 10% glycerol, 1% NP-40 and freshly added 1 mM DTT, protease inhibitor cocktail (Sigma) and phosphatase inhibitor cocktails (Sigma)), sonicated and cleared from debris by high-speed centrifugation. For IP, nuclei were lysed in buffer 4 (450 mM NaCl, 20 mM HEPES pH 7.5, 1 mM $MgCl_2$, 0.5 mM EDTA, 0.5 mM EGTA, 10% glycerol, 0.3% Triton X-100 and freshly added 1 mM DTT, protease inhibitor cocktail (Sigma) and phosphatase inhibitor cocktails (Sigma)), and cleared from debris by high-speed centrifugation. Buffer 4 without the preceding fractionation steps was also used for preparation of whole cell lysates. Prior to IP, salt and detergent concentrations in whole cell and nuclear extracts were adjusted to 150 mM NaCl and 0.1% Triton X-100, respectively. Lysates were pre-cleared with GammaBind G Sepharose (GE Healthcare) and incubated with primary antibody against Cry1, Bmal1, Clock (all rabbit polyclonal, Bethyl Laboratories) or K538 Acetyl-Bmal1 (rabbit polyclonal, Millipore). Rabbit polyclonal anti-Nfx1 antibody (Bethyl Laboratories) was used as isotype negative control. Immune complexes were precipitated with GammaBind G Sepharose (GE Healthcare), washed in buffer 5 (as IP buffer except with a higher detergent concentration of 0.3% Triton X-100) and analyzed by SDS-PAGE and Western Blot. Western Blotting was performed according to standard procedures using the above described antibodies as well as anti-Per2 (rabbit polyclonal, Alpha Diagnostics) anti-TATA binding protein TBP (mouse monoclonal, Abcam) and anti-α-Tubulin (mouse monoclonal, Sigma). Note on K538 Acetyl-Bmal1 antibody: Due to differences in residue numbering between Bmal1 splice variants, K538 in the reference sequence used by the vendor (Uniprot O00327-2) corresponds to the K537 residue for which acetylation has been described (Czarna et al., 2011; Hirayama et al., 2007). Blots were quantified using ImageJ and statistical significance was tested using paired t tests in Prism 5 (GraphPad Software).

Clock Gene Expression Analysis

Total RNA was prepared from CRY1 fl or Δ11 MEFs using the RNeasy mini kit with on-column DNase digestion (QIAGEN). Equal amounts of total RNA were used for first-strand cDNA synthesis using the SuperScript III First-Strand Synthesis System with random hexamer priming followed by RNase H digestion (Invitrogen, Life Technologies). Diluted first-strand cDNA was used as template in quantitative real-time PCR reactions using the LightCycler 480 SYBR Green I Master kit (Roche) and the oligos listed in Table S3. Triplicate reactions for each sample and primer set were run on a LightCycler 480 instrument (Roche). Samples were quantified relative to a standard curve prepared from serial dilutions of concentrated cDNA run in parallel using the second derivative maximum method in LightCycler 480 instrument software (version 1.5, Roche). Relative transcript levels were normalized to *Tbp* values and expressed as fold change relative to the mean of the entire data series combining both genotypes. Statistical significance in mean transcript expression levels between genotypes from five independent experiments was assessed by appropriate curve fitting and comparing the best-fit-values between datasets by extra sum-of-squares F test in Prism 5 (GraphPad Software). For curve fitting, a standard sine curve modified to allow for translation along the y axis (Y = Amplitude*sin((2*pi*X/Wavelength)+PhaseShift)+B) was used for oscillating transcripts and a horizontal line (Y = Mean) was used for the non-circadian control transcript.

Chromatin Immunoprecipitation

For dual crosslinking, cells were treated with 2 mM EGS (Thermo Scientific) for 20 min in PBS to which 1% Formaldehyde was added for another 8 min. To stop the reaction, 156.25 mM glycine was added and incubation was continued for another 10 min. Cells were washed in ice-cold PBS and lysed in cytoplasmic lysis buffer (320 mM sucrose, 10 mM Tris-HCl pH 8.0, 3 mM $CaCl_2$, 2 mM Mg Acetate, 0.1 mM EDTA, 0.5% NP-40). Nuclei were collected and washed as described above and dry pellets were stored at −80°C until further use. For chromatin immunoprecipitation (ChIP), nuclei were resuspended in ChIP lysis buffer (10 mM Tris-HCl pH 8.0, 150 mM NaCl, 1 mM EDTA, 1% Triton X-100, 0.1% sodium deoxycholate, 0.25% *N*-lauroylsarcosine and freshly added protease inhibitor cocktail (Sigma)) and sonicated in a Bioruptor Pico (Diagenode) for 20 30 s cycles. Sonicated lysates were cleared by high-speed centrifugation and an aliquot was removed and saved as the input sample. The remaining lysate was used undiluted for CRY1 ChIP or diluted with ChIP buffer as follows: 1:3.33 for Bmal1 and Clock ChIP and 1:5 for H3K4me3 ChIP. Lysates were pre-cleared with Protein A/G Plus-agarose (Santa Cruz) that had been pre-blocked with 5mg/ml BSA. Pre-cleared lysates were incubated with antibody overnight at 4°C. Antibodies were as described above and Trimethyl-Histone H3 (Lys4) antibody was from Millipore. Immune complexes were collected with Protein A/G agarose beads and washed three times in ChIP lysis buffer, three times in LiCl wash buffer (20 mM Tris-HCl pH 7.5, 250 mM LiCl, 2 mM EDTA, 0.5% IGEPAL CA-630, 1% sodium deoxycholate, 1mM PMSF) and once in TE (10 mM Tris-HCl pH 8.0, 1 mM EDTA). Beads were incubated with elution buffer (20 mM Tris-HCl pH 8.0, 5 mM EDTA, 0.5% sodium dodecyl sulfate) for 30 min at 65°C under agitation. ChIP eluates and saved input samples were reverse cross-linked at 65°C overnight and treated with 1 μg RNase (Roche) for 1 hr at 37°C and 200 μg proteinase K (Roche) for 2 hr at 55°C. DNA was purified using commercial spin columns. The amount of *Per2*, *Dbp* and *Lrwd1* promoter DNA in ChIP samples and 1/50-diluted input samples was measured by quantitative real-time PCR as above using the oligos listed in Table S3. Triplicate reactions for each sample and primer set were run on a LightCycler 480 instrument (Roche) and quantified relative to a standard curve prepared from serial dilutions of input DNA run in parallel. PCR results were adjusted for any applicable prior dilutions and results from ChIP samples were normalized to the result of the respective input sample. For comparison between genotypes, results are expressed as fold change in the CRY1 Δ11 sample compared to the CRY1 full-length sample, which was set to 1.

Luciferase Repression Assay

Human *CLOCK* and *ARNTL* cDNAs were PCR amplified from first-strand cDNA libraries derived from human fibroblast cell lines and blunt-cloned into the EcoRV-site of pBluescript. Sequences were confirmed by Sanger-sequencing. *CLOCK* and *ARNTL* ORFs were subcloned in frame into a modified pcDNA3.1 vector (Invitrogen, Life Technologies) containing an N-terminal Flag-tag using EcoRV/NotI restriction sites.

293T cells were transiently transfected with 0.5 ng phRG-TK (renilla-luc, kind gift of S. Stanley), 5 ng pGL3-AVP (Kume et al., 1999), 125 ng pcDNA3-Flag-Clock, 125 ng pcDNA3-Flag-Bmal1 and 125 ng to 1 ng pcDNA3-HA-Cry1fl or Δ11 using Lipofectamin 2000 (Invitrogen, Life Technologies). DNA amounts were adjusted to a total of 500 ng per transfection with empty pcDNA3. Transcriptional activity was assessed 48 hr post transfection by measuring the firefly/renilla luciferase ratio in cell lysates using a Dual-Luciferase Reporter Assay System (Promega) and single tube luminometer (Berthold Detection Systems).

Cry DKO MEFs were transfected with 250 ng pGL3-Per2dLuc (Ueda et al., 2002) and 750 ng of lentiviral vectors pLV6puro-hCry1fl, -Δ11, mCry2 or empty vector and transcriptional activity was assessed as above.

Luciferase Stability Assay

Vectors encoding C-terminal luciferase fusions of CRY1 fl and Δ11 (pcDNA3F-hCry1-luc) were generated by first cloning the respective open reading frames without the final stop codon into a modified pcDNA3.1 vector (Invitrogen, Life Technologies) containing an N-terminal Flag-tag using EcoRV/NotI restriction sites. The luciferase ORF was amplified from pGL3 and cloned in frame into the above CRY1 constructs using NotI/XbaI restriction sites. 293T cells were seeded in 35-mm plates and transfected with 1 μg pcDNA3F-hCry1-luc (fl or Δ11) and 3 μg empty pcDNA3 vector using Lipofectamin 2000 (Invitrogen, Life Technologies). 48 hr after transfection the medium was changed to counting medium (phenol red- and L-glutamine-free DMEM (GIBCO), 100 U/ml penicillin and 100 μg/ml streptomycin, 10% FBS, 10 mM HEPES pH 7.2 (GIBCO), 2 mM L-glutamine (GIBCO), 0.5 mM firefly D-luciferin potassium salt (Biosynth)). Cycloheximide was added to a final concentration of 20 μg/ml and luminescence was recorded every 15 min in a LM-2400 bioluminescence detection system (Hamamatsu) for 24 hr. For analysis, raw luminescence data were normalized to the peak value of each sample and half-life was determined by fitting one-phase decay curves in Prism 5 (GraphPad Software).

QUANTIFICATION AND STATISTICAL ANALYSIS

Where applicable, statistical parameters including sample size, precision measures (standard error or standard deviation) and statistical significance are reported in the Figures and corresponding Figure Legends.

Data Analysis for Human In-Laboratory Study

For sleep data analysis, PSG TWin 4.1. software (Grass Technologies, Natus Neurology, West Warwick, RI) was used for scoring electrographic recordings in 30 s epochs according to standard AASM criteria for N1, N2, N3, REM or wake. A list of sleep-stage/wake status per epoch was created from the exported notations file of each scored record. Gaps within or between records were treated as 'wake', if the laboratory technician log indicated that the subject was awake during this time. Any gaps occurring within a sleep episode were regarded as sleep (without stage assignment) until indicated otherwise by the log. Analysis of circadian rhythmicity during the free-run was conducted using X^2 periodogram and fast Fourier transform (FFT) functions on 2 min-binned data for period and amplitude analyses, respectively, in ClockLab (ActiMetrics, Wilmette, IL).

For analysis of core body temperature data, raw data were corrected for non-physiological outliers associated mostly with replacement of the ingestible temperature sensor in the following way: Data were excluded, if they were outside of a lower or upper threshold or if the difference between two adjacent points was more than 0.1°C. Remaining outliers were removed manually upon visual inspection of the temperature trace (see Figure S1). Data gaps were bridged by linear interpolation between the last and next available point. Analysis of circadian rhythmicity during the free-run was conducted in ClockLab (ActiMetrics, Wilmette, IL) on outlier-corrected, interpolated, 2 min-binned data. Period was derived from X^2 periodogram. Data were mean-subtracted prior to determination of amplitude by FFT.

Data Analysis for Whole Exome Sequencing

Sequences were aligned to human genome build GRCh37 using BWA (Burrows-Wheeler Aligner) (Li and Durbin, 2009). Duplicate reads were marked using Picard (http://picard.sourceforge.net). GATK (Genome Analysis Toolkit) (DePristo et al., 2011) was used for base quality score recalibration (BQSR) and local realignment around indels to refine alignment artifacts around putative insertions or deletions. Variant discovery was performed in two steps - variant calling with GATK HaplotypeCaller followed by joint genotyping using GATK GenotypeGVCFs. The resulting variant call set was refined using Variant Quality Score Recalibration (VQSR) as implemented in GATK VariantRecalibrator. The VQSR scores were used to define low quality variants for downstream processing. SnpEff (Cingolani et al., 2012) and VCFtools (Danecek et al., 2011) were used to add variant effect predictions and functional annotations.

Potentially functional genetic variants co-segregating with the sleep phenotype were identified by WES of four affected and one unaffected family member, as described above. After filtering, 33 candidate variants remained (Table S2). Of these variants, only CRY1 c.1657+3A>C potentially affected a gene with a possible role in sleep or circadian rhythm. While not excluding the possibility

that a variant in a previously uncharacterized gene could be causal for the sleep phenotype, we decided first to carry out experimental characterization of the CRY1 variant.

Cellular Period Analysis

Period analysis was performed by fitting a damped sine curve to time series data detrended by subtracting a running average using Lumicycle analysis software (Actimetrics). Goodness-of-fit values for curve fitting were routinely above 90%. Statistical significance between genotypes was assessed using an unpaired t test.

Association between CRY1 c.1657+3A>C Genotype and Sleep Behavior

Subjects were classified into the following behavioral categories: affected late, affected fragmented, probably affected, probably not affected, not affected or uninterpretable. Factors that contributed to the classification of each subject are listed in Table S1. For the statistical analysis of the association between sleep behavior and *CRY1* allele status, the first three categories were combined as 'affected' and the third and fourth category were combined as 'unaffected'. Subjects deemed 'uninterpretable' were excluded from the analysis. Total subject numbers for the individual categories were as follows:

	Affected	Non-affected	Total
Carrier (C/C or +/C)	44	1	45
Non-carrier (+/+)	0	32	32
Total	44	33	77

P value from Fisher's exact test, odds ratio and 95% confidence interval were calculated in Prism 5 (GraphPad Software).

Analysis of Western Blot Data

Blots were quantified using ImageJ and statistical significance was tested using paired t tests in Prism 5 (GraphPad Software).

Analysis of Clock Gene Expression Data

Triplicate PCR reactions for each sample and primer set were run on a LightCycler 480 instrument (Roche). Samples were quantified relative to a standard curve prepared from serial dilutions of concentrated cDNA run in parallel using the second derivative maximum method in LightCycler 480 instrument software (version 1.5, Roche). Relative mRNA levels were normalized to *Tbp* values and expressed as fold change relative to the mean of the entire data series combining both genotypes. Statistical significance in mean transcript expression levels between genotypes from five independent experiments was assessed by appropriate curve fitting and comparing the best-fit-values between datasets by extra sum-of-squares F test in Prism 5 (GraphPad Software). For curve fitting, a standard sine curve modified to allow for translation along the y axis (Y = Amplitude*sin((2*pi*X/Wavelength)+PhaseShift)+B) was used for oscillating transcripts and a horizontal line (Y = Mean) was used for the non-circadian control transcript.

Analysis of ChIP Data

Triplicate PCR reactions for each sample and primer set were run on a LightCycler 480 instrument (Roche) and quantified relative to a standard curve prepared from serial dilutions of input DNA run in parallel. PCR results were adjusted for any applicable prior dilutions (see Method Details) and results from ChIP samples were normalized to the result of the corresponding input sample. For comparison between genotypes, results are expressed as fold change in the CRY1 Δ11 sample compared to the CRY1 full-length sample, which was set to 1. Average results from three independent experiments are shown.

DATA AND SOFTWARE AVAILABILITY

Further information and requests for raw data, analysis details, and DNA samples may be directed to and fulfilled in compliance with IRB protocol requirements by Lead Contact Michael W. Young (young@rockefeller.edu), or for Turkish subjects by Tayfun Ozcelik (tozcelik@bilkent.edu.tr). Whole exome sequencing data are not deposited in a public repository because the genetic sharing plans of the IRB approved consent forms used in this study do not permit the deposition of such data into public or controlled-access databases.

Cell

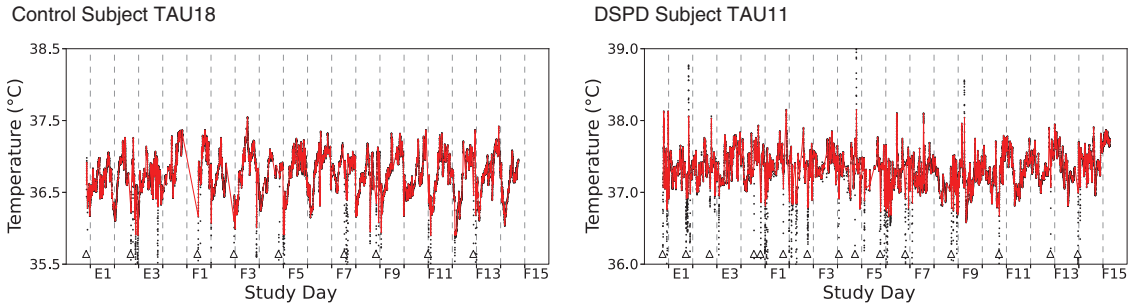

Figure S1. Core Body Temperature Rhythms of Control Subject TAU18 and the Proband TAU11, Related to Figure 2

Overlay of raw core body temperature readings (black dots) with outlier-corrected, interpolated data (red line). Sequential study days from entrainment day 1 (E1) to the final free-run day (F15) are plotted on the x axis. White triangles indicate replacement of the ingestible temperature sensor.

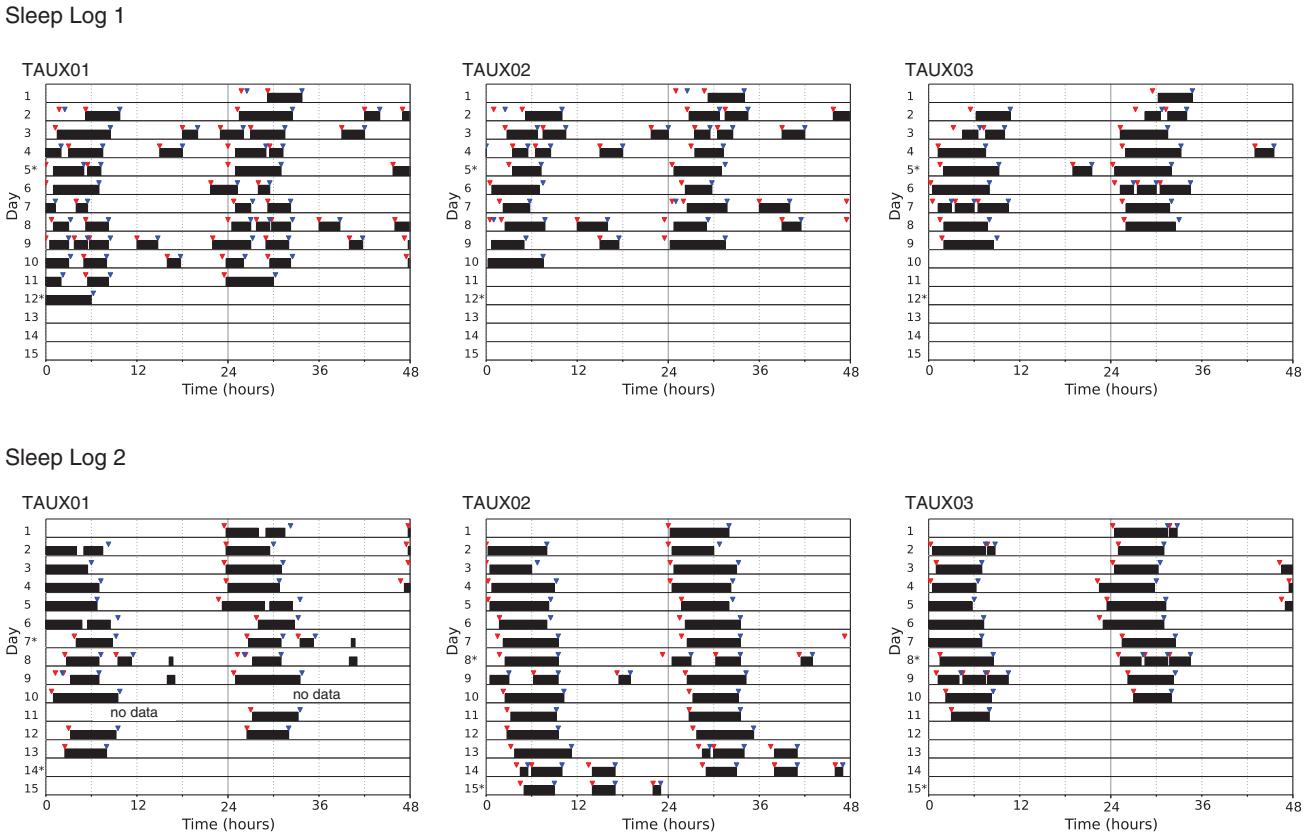

Figure S2. Double-Plotted Sleep Log Data of Proband Family Members TAUX01–03, Related to Figure 4 and Table S1

Red and blue triangles indicate in-bed/out-of-bed times, respectively. Black bars represent the self-estimated time asleep. Asterisks indicate Sundays. Upon completion of sleep log 1, subjects TAUX01 and TAUX02 disclosed a necessity for early rising during the recorded period for reasons unrelated to the study and indicated that data were not representative of their usual sleep-wake schedule. Subjects were therefore asked to repeat the data collection (sleep log 2). Data from sleep log 1 are shown to illustrate features of abnormal sleep timing despite early wake times.

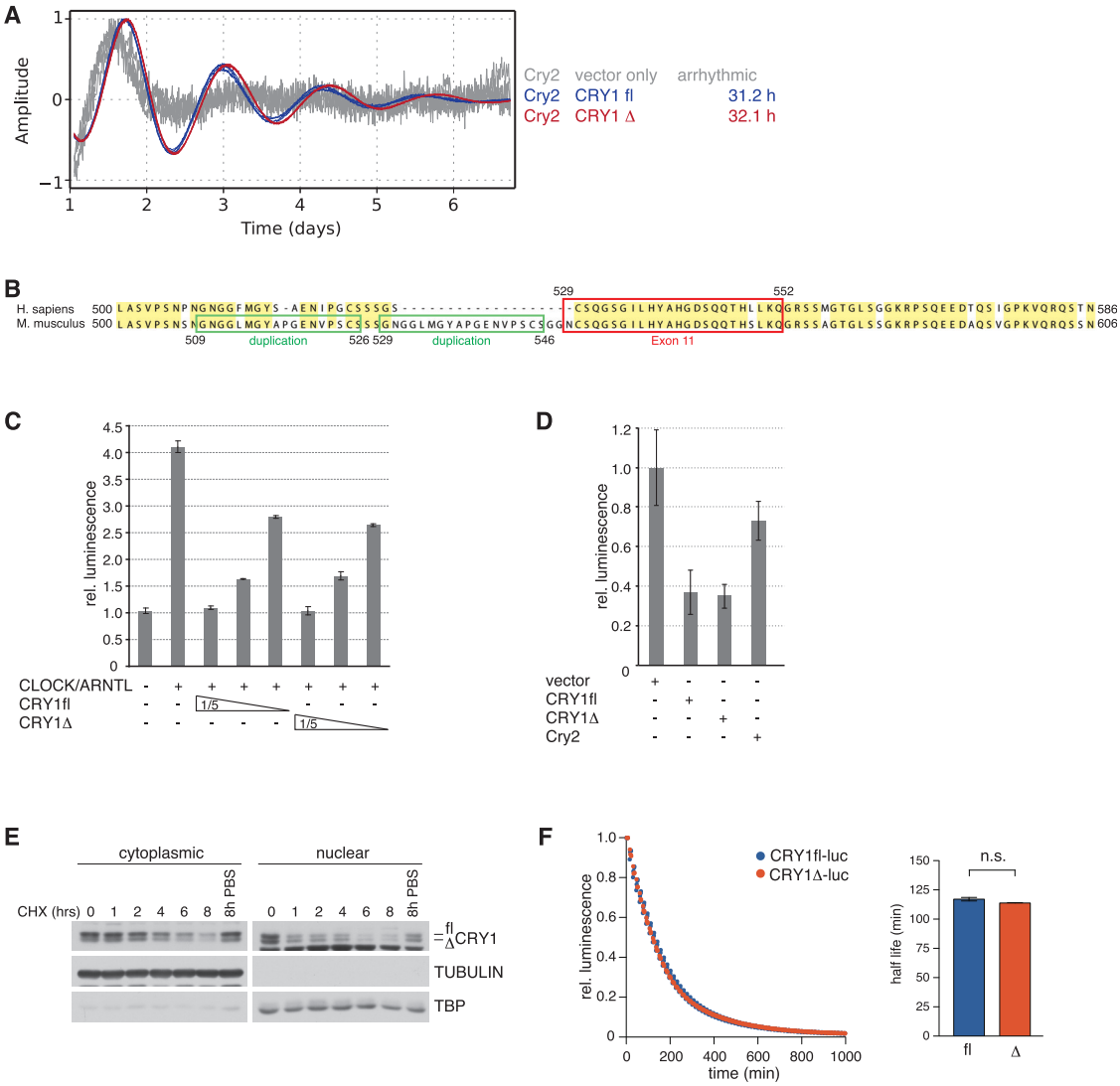

Figure S3. Effect of Exon 11 Deletion on CRY1 Function, Related to Figures 4 and 6

(A) Bmal-luc expression of Cry DKO MEFs reconstituted with lentiviral Cry2 and either empty vector or CRY1 fl or Δ11. All Cry forms were expressed using regulatory elements previously characterized to recapitulate endogenous Cry1 oscillation (Ukai-Tadenuma et al., 2011). Cells were synchronized with 20 μM forskolin and bioluminescence output was recorded for approximately seven days. Traces show detrended bioluminescence counts normalized to the first peak for each genotype (Cry2 and vector control: gray, Cry2 and CRY1 fl: blue, Cry2 and CRY1 Δ11: red). Period for the latter two represents the average from quadruplicate samples.

(B) Sequence comparison of the human and murine CRY1 tail. Identical residues are shaded in yellow. Preceding exon 11, murine Cry1 contains a 19-residue insertion that is not present in human CRY1.

(C) Inhibition of Clock/Bmal1-dependend transcription by fl and Δ11 CRY1. An E-box-driven luciferase reporter plasmid AVP-luc was co-expressed in 293T cells along with CLOCK, ARNTL and decreasing amounts of CRY1 fl or Δ11 as indicated. Data represent the mean induction of bioluminescence over basal levels from duplicate transfections at 48 hr post-transfection. Error bars represent the standard deviation from duplicate samples.

(D) Transcriptional inhibition in Cry DKO cells transiently transfected with Per2-dLuc and either empty vector or a lentiviral vector encoding CRY1 fl, CRY1 Δ11 or Cry2 under control of a physiological Cry1 promoter (Khan et al., 2012). Data represent the mean induction of bioluminescence from quadruplicate transfections at 48 hr post-transfection. Error bars represent the standard deviation from quadruplicate samples.

(E) Protein stability of CRY1 fl and Δ11. Proband fibroblasts were treated with 20 μg/ml cycloheximide (CHX) for the indicated times or with solvent control. CRY1 levels were measured by Western Blot in fractionated cytoplasmic and nuclear extracts with TUBULIN and TBP used as controls for protein loading and fractionation purity.

(F) Luciferase fusion proteins of fl and Δ11 CRY1 were transiently expressed in 293T cells. Cells were treated with 20 μg/ml CHX and luminescence was recorded over time. For analysis, raw luminescence data were normalized to the peak value of each sample and half-life was determined by fitting one-phase decay curves in Prism 5 (GraphPad Software). Error bars represent the standard error from quadruplicate samples.

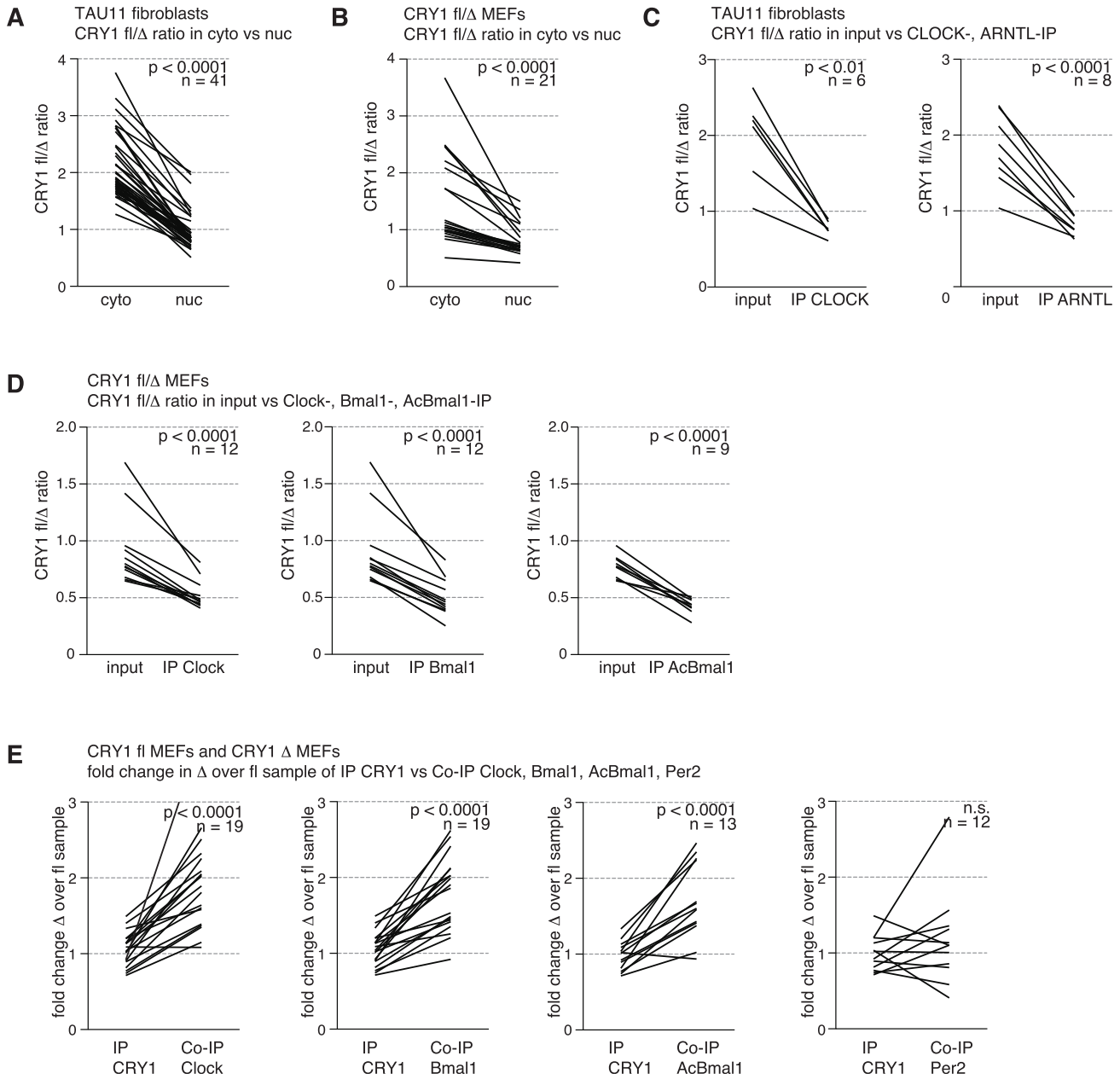

Figure S4. Effect of Exon 11 Deletion on CRY1 Function, Related to Figure 6

(A–E) Quantification of findings reported in Figure 6. Plotted data include exact experiments from Figure 6 as well as independent replications. Individual panels combine data derived from both synchronized and unsynchronized cells and, for (C–E), immunoprecipitations performed on whole cell and nuclear extracts. Sample size and statistical significance as determined by paired t test are included in each panel. (A) Ratio of CRY1 full-length to CRY1 Δ11 expression in cytoplasmic versus nuclear extracts from TAU11 fibroblasts. (B) Ratio of CRY1 full-length to CRY1 Δ11 expression in cytoplasmic versus nuclear extracts from CRY1 fl/Δ MEFs. (C) Ratio of CRY1 full-length to CRY1 Δ11 co-immunoprecipitating with CLOCK or ARNTL compared to the lysate input prepared from TAU11 fibroblasts. (D) Ratio of CRY1 full-length to CRY1 Δ11 co-immunoprecipitating with Clock, Bmal1 or Acetyl-Bmal1 compared to the lysate input prepared from CRY1 fl/Δ MEFs. (E) Full-length or Δ11 CRY1 were immunoprecipitated from MEFs expressing either CRY1 form. Data show the fold change in the CRY1 Δ11 sample over the CRY1 full-length sample for CRY1 and co-immunoprecipitating Clock, Bmal1, Acetyl-Bmal1 and Per2.

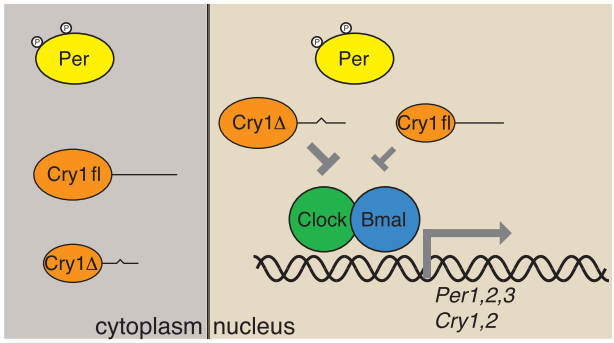

Figure S5. Mechanism of Circadian Clock Regulation by CRY1 Δ11, Related to Figures 6 and 7

Deletion of exon 11 leads to enhanced CRY1 nuclear localization, interaction with transcription factors Clock/Bmal1, their displacement from DNA and repression of target genes.